Distribution Category
Physics—General (UC-34)

ANL-83-18

ANL--83-18

DE83 010692

ARGONNE NATIONAL LABORATORY
9700 South Cass Avenue
Argonne, Illinois 60439

EXPERIMENTS ON TUBES CONVEYING FLUID

by

J. A. Jendrzejczyk and S. S. Chen

Components Technology Division

February 1983

TABLE OF CONTENTS

LIST OF ILLUSTRATIONS

LIST OF TABLES

EXPERIMENTS ON TUBES CONVEYING FLUID

by

J. A. Jendrzejczyk and S. S. Chen

ABSTRACT

Tests are conducted for tubes conveying fluid for six types of support conditions. The objectives are to understand the dynamic characteristics of such systems for different support conditions and to explore the methods to control tube stability. Transition from one instability mechanism to another is examined, and the feasibility of using feedback control to increase the critical flow velocity is demonstrated.

I. INTRODUCTION AND OBJECTIVES

Within a program sponsored by the Department of Energy, Office of Basic Energy Sciences, theoretical and experimental studies are being integrated with the objectives of enhancing the understanding of nonlinear stability phenomena involving fluids, solids, and their coupling; developing methods of controlling instability; and exploring the use of instability mechanism in engineering design. These studies have been initiated with the special fluidelastic instability problem of a slender elastic tube conveying fluid. The results of an initial series of tests involving tubes conveying fluid are reported here.

The dynamics of tubes conveying fluid is an academically interesting and practically important problem. Many studies have been published on the subject; e.g., see Refs. 1 and 2 for brief reviews. Most of the investigations are analytical studies with the objective of quantifying the effect of various system parameters. There have been fewer experimental studies; experimental investigations are listed in Table 1 (Refs. 3-14).

A successful experiment on the instability of tubes conveying fluid is, by no means, trivial. As shown in Table 1, a successful test will require a high-pressure loop for metal tubes with high flexural rigidity, while with a low-pressure loop, tubes of rubber, plastic, or other materials with very low flexural rigidity are required. In some experiments, no instability is observed because of the limitations of the available equipment. A high-pressure loop is relatively expensive, while for a low-pressure loop, the material properties are much more difficult to control and the initial imperfection may affect the instability boundaries. A means to alleviate the problem is to use articulated pipes (Refs. 15-17). However, the

Table 1. A List of Experimental Studies on Tubes Conveying Fluid

Authors	Tube Material	Fluid	Support Condition	Tube Orientation	Instrumentation	Measured Parameters	Instability Type	Remarks
Long (1955)	Steel tubes	Water	Hinged-Hinged, Fixed-Free, Fixed-Fixed	Horizontal	Strain gauges	Damping. Frequency		Flow velocity is low; no instability occurs.
Gregory and Paidoussis (1961)	1. Rubber tubes 2. Metal tubes	1. Water and air 2. Oil (high pressure)	Fixed-Free	Horizontal	Camera	Critical flow velocity. Frequency and mode at instability	Flutter	Nozzle is attached to the free end in some cases.
Dodds et al. (1965)	Aluminum alloy	Water (high pressure)	Hinged-Hinged	Horizontal	Strain gauges	Tube displacement. Critical flow velocity, Tube frequency and damping	Divergence	
Greenwald and Dugundji (1967)	Elastomeric and polyethylene tubes	Water	1. Fixed-Free 2. Fixed-Hinged	Hanging vertically	Strain gauges	Critical flow velocity. Frequency and mode at instability	1. Flutter 2. Divergence	
Naguleswaran and Williams (1968)	Neoprene tube	Water	Fixed-Fixed	Horizontal	Capacitance pickups	Frequency		No buckling is observed because of nonlinear effects
Paidoussis (1970)	Rubber tubes	Air or water	Fixed-Free	Standing and hanging vertically	Fiber optics	Critical flow velocity. Frequency and mode at instability	Divergence and flutter	

Table 1. A List of Experimental Studies on Tubes Conveying Fluid (Contd.)

Authors	Tube Material	Fluid	Support Condition	Tube Orientation	Instrumentation	Measured Parameters	Instability Type	Remarks
Hill and Swanson (1970)	Latex surgical tubes	Water	Fixed-Free			Critical flow velocity and frequency at instability		Lumped masses attached to the tubes
Liu and Mote (1973)	Aluminum	Oil (high pressure)	Fixed-Free, Fixed-Fixed, Fixed-Hinged	Hanging vertically	Strain gauges and accelerometers	Natural frequency. Static displacement		No instability is observed because of nonlinear effects
Paidoussis and Issid (1976)	Silicon rubber tubes	Water	Fixed-Free, Fixed-Fixed	Hanging vertically		Boundaries of parametric resonance	Parametric resonance	Tubes conveying pulsating flow
Becker et al. (1978)	Plastic drinking straws	Air	Fixed-Free		Stroboscope	Critical flow velocity. Frequency and mode at instability	Flutter	
Hannoyer and Paidoussis (1979)	Silicon rubber tubes	Water	Fixed-Free	Hanging vertically		Flow velocity and oscillation frequency at instability	Flutter	Tapered tubes
Shilling and Lou (1980)	PVC pipes	Water	Fixed-Free	Hanging vertically	Accelerometers	Frequency and tube response spectra to forced excitation		No instability is observed because of the limitations of equipment availability. Lumped masses attached to the tubes

characteristics of an articulated tube are not necessarily the same as those of a continuous tube.[17]

The dynamic characteristics of a tube conveying fluid vary with support conditions. For example, a cantilevered tube will lose stability by flutter,[4,6] while a simply supported tube will lose stability by divergence.[5] The effect of flow velocity on vibrational characteristics, such as natural frequency, mode shape, and damping, are also different for different end conditions. In summary, tube-support condition plays an important role. The first objective of this study is to compare the dynamic response characteristics of tubes supported by different conditions.

Most of the investigations are confined to establishing the critical flow velocity at which large tube displacement develops. In general, the critical flow velocity is very high and is of no great concern in practice. The vibrational characteristics at subcritical flow-velocity ranges are much more important for most practical applications. Therefore, the second objective of this experiment is to investigate the response of tubes in the low (subcritical) flow-velocity range.

The instability mechanism may vary with a small change of a certain system parameter. For example, a cantilevered tube conveying fluid, which is stable at a given flow velocity, can be made to become unstable by simply touching it at the free end, which in effect changes the boundary condition. In addition, different instability regions may be associated with different instability mechanisms. The third objective is to demonstrate the transition of different instability mechanisms by varying a particular system parameter.

Tubes conveying fluid may be stabilized or destabilized by changing system parameters or by applying external excitations. The fourth objective is to explore methods to control system stability. The stabilization technique will be useful not only for tubes conveying fluid but also for other problems such as the control of the transition from laminar to turbulent flow.[18]

Tests are performed for six different support conditions: Case 1: fixed-free tubes; Case 2: tubes fixed at the upstream end and supported by an elastic spring at the downstream end; Case 3: a fixed-fixed tube; Case 4: tubes with a fixed support at the upstream end and a "knife-edge" support movable along the tube; Case 5: a tube fixed at the upstream end and a weight attached to the downstream end; and Case 6: a tube fixed at the upstream end, a weight attached to the downstream end, and an additional weight movable along the tube. Note that Cases 1, 5, and 6 correspond to a nonconservative system, Case 3 corresponds to a gyroscopic conservative system, and Cases 2 and 4 can be a nonconservative or gyroscopic conservative system depending on the spring constant in Case 2 and the location of the movable support in Case 4. Results of these tests provide additional insight into the dynamics of tubes conveying fluid and demonstrate a method to control stability.

II. TEST EQUIPMENT AND PROCEDURES

A general view of the test section is shown in Fig. 1. The test section is connected to a 0.052-m^3/s (700-gpm) water loop. The water flows from an accumulator through the pump, a 10.2-cm (4-in.) flowmeter, a pneumatic control valve, and a 6.35-cm (2.5-in.)-ID flexible hose, which is connected to the test specimen with an adapter. The tube is mounted vertically so that the water discharges downward into a 208-liter (55-gal) reservoir. A pump returns the water to the accumulator.

To measure damping, and also as a means of controlling stability, the tube is excited with a small electromagnetic exciter consisting of permanent magnets mounted on the specimen and two coils mounted to a plate near the tube. (See Fig. 2 for a typical setup.)

Tubes of two different materials are used in the experiments: polyethylene and acrylic. The nominal tube outside diameters are 0.95 cm (0.375 in.), 1.27 cm (0.5 in.), and 1.59 cm (0.625 in.), all with a 0.159-cm (0.0625-in.) wall thickness. Young's modulus is determined experimentally from the frequency of a cantilevered tube with various lengths; it is 2.87×10^8 Pa (4.16×10^4 psi) for polyethylene tubes and 3.58×10^9 Pa (5.2×10^5 psi) for acrylic tubes. Tube density is 9.45×10^{-3} N/cm^3 (0.0348 lb/$in.^3$) for polyethylene tubes and 0.0115 N/cm^3 (0.0424 lb/$in.^3$) for acrylic tubes.

Tubes with six different supported conditions are tested (see Fig. 3):

Case 1: Fixed-free tubes.

- Test 1.1 - polyethylene tube, 60.96 cm (24 in.) long, and 0.95-cm (0.375-in.) OD.
- Test 1.2 - polyethylene tube, 60.96 cm (24 in.) long, and 1.27-cm (0.5-in.) OD.
- Test 1.3 - polyethylene tube, 60.33 cm (23.75 in.) long, and 1.59-cm (0.625-in.) OD.
- Test 1.4 - acrylic tube, 1.30 m (51 in.) long, and 0.95-cm (0.375-in.) OD.
- Test 1.5 - acrylic tube, 1.30 m (51 in.) long, and 1.27 cm (0.5 in.) OD.
- Test 1.6 - acrylic tube, 1.30 m (51.1 in.) long, and 1.59 cm (0.625 in.) OD.

Case 2: Tubes fixed at the upstream end and supported by an elastic spring at the downstream end.

- Test 2.1 - polyethylene tube, 60.96 cm (24 in.) long, 1.27-cm (0.5-in.) OD, and spring constant 0.193 N/cm (0.11 lb/in.).

Fig. 1. Test Equipment. ANL Neg. No. 113-5338.

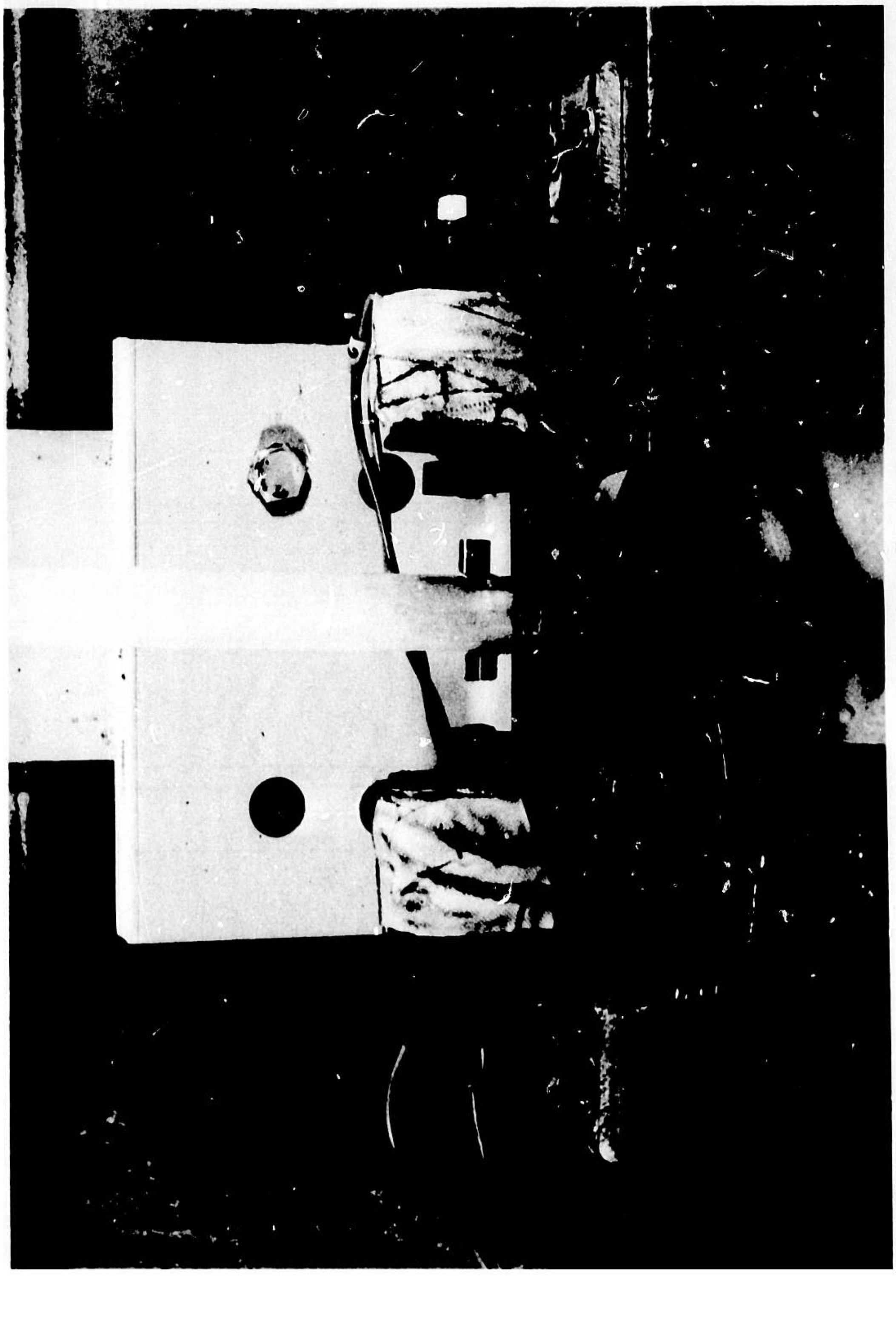

Fig. 2. Electromagnetic Excitation Assembly. ANL Neg. No. 113-5340.

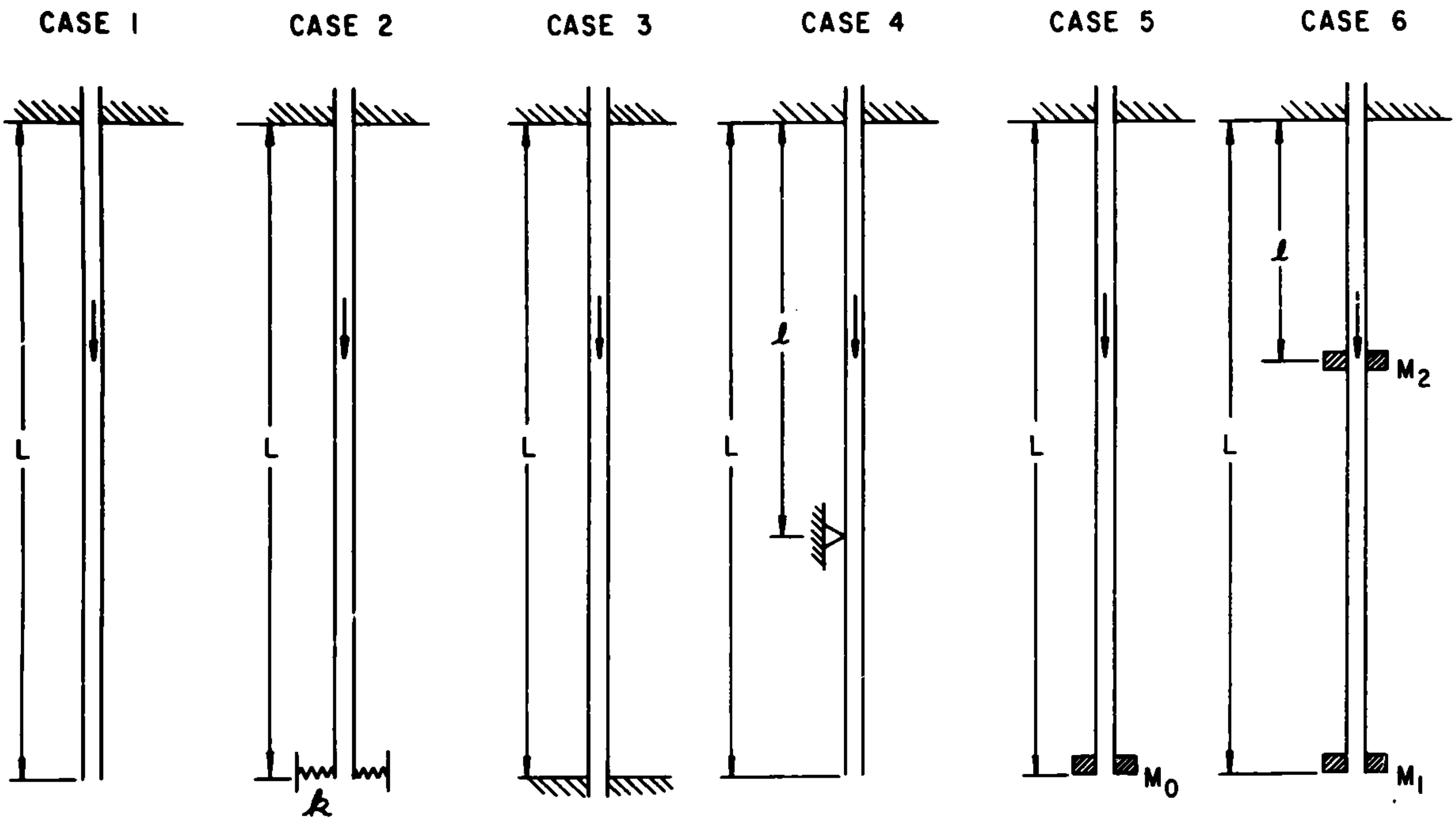

Fig. 3. Six Test Cases

- Test 2.2 - polyethylene tube, 60.96 cm (24 in.) long, 1.27-cm (0.5-in.) OD, and spring constant 0.876 N/cm (0.5 lb/in.).

Case 3: A fixed-fixed acrylic tube, 130 cm (51 in.) long, and 0.95-cm (0.375-in.) O.D.

Case 4: Tubes fixed at the upstream end and a knife-edge support movable along the tube.

- Test 4.1 - polyethylene tube, 68.58 cm (27 in.) long, 0.95-cm (0.375-in.) OD, and ℓ/L = 0, 0.120, 0.194, 0.266, 0.342, 0.417, 0.488, 0.563, 0.634, 0.711, 0.787, 0.861, and 0.935.
- Test 4.2 - polyethylene tube, 90.2 cm (35.5 in.) long, 1.27-cm (0.5-in.) OD, and ℓ/L = 0, 0.069, 0.120, 0.193, 0.368, 0.424, 0.481, 0.593, 0.650, 0.706, 0.762, 0.875, 0.933, and 0.986.

Case 5: An acrylic tube, 152.4 cm (60.0 in.) long and 0.95-cm (0.375-in.) OD.

- Test 5.1 - M_0 = 4 N (0.899 lb), a brass cylinder 3.18-cm (1.25-in.) OD, 0.95-cm (0.375-in.) ID, and 6.51 cm (2.56 in.) long.
- Test 5.2 - M_0 = 4.06 N (0.912 lb), a brass cylinder 3.18-cm (1.25-in.) OD, 0.95-cm (0.375-in.) ID, 6.83 cm (2.69 in.) long, with six sets of small permanent magnets imbedded in it.

Case 6: An acrylic tube, 115.6 cm (45.5 in.) long and 1.27-cm (0.5-in.) OD.

M_1 = 4.48 N (1.007 lb), a brass cylinder 3.18-cm (1.25-in.) OD, 1.27-cm (0.50-in.) ID and 7.78 cm (3.06 in.) long.

M_2 = 2.09 N (0.47 lb), a brass cylinder 3.18-cm (1.25-in.) OD, 1.27-cm (0.50-in.) ID and 3.81 cm (1.5 in.) long, with magnets imbedded in it.

The spring used in Case 2 is mounted to the downstream end with a ring as shown in Fig. 4. Four springs of equal stiffness mounted 90° apart provide the same stiffness in all directions.

Pressure drop through the test specimen is measured using a pressure gauge connected to the pressure tap at the tube adapter. A flowmeter measures the flow velocity through the tube. For each test specimen, the relation between the flow velocity and the pressure drop was established; the flow velocity can then be determined from the pressure readings.

Displacements of the tubes are measured with optical trackers. Two optical trackers are used for Cases 1-3 and one for Cases 4-6. The displacements are measured at different locations:

- Cases 1 and 2: the downstream end.

Fig. 4. Elastic Support at the Downstream End for Case 2. ANL Neg. No. 113-5341.

- Case 3: the midspan.
- Case 4: the downstream end for $\ell/L < 0.4$ and the midspan between the supports for $\ell/L > 0.4$.
- Case 5: 36.2 cm (14.25 in.) from the fixed end.
- Case 6: 13.5 cm (5.32 in.) from the fixed end.

The displacement signals are analyzed for their static deflection and rms component. From the frequency spectra, the dominant frequencies of tube response can be identified.

Damping of the tube is determined using the log decrement of tube displacement to an impact, or the bandwidth method using the magnet-coil exciter.

In Test 5.2, a series of small permanent magnets is imbedded in the attached weight. This allows an external force to be applied using the electromagnetic exciter assembly. This exciter is used for several tests: (a) swept-sine excitation to obtain natural frequency and modal damping ratio; (b) a sinusoidal force applied to the tube to investigate the feasibility of stability control using a mechanical excitation force; and (c) a feedback excitation applied to the tube to investigate the role of feedback-control system.

In Case 6, the mass M_2 can be located at different positions denoted bv ℓ. The critical flow velocity is determined as a function of the ratio ℓ/L.

III. RESULTS

A. Case 1: Fixed-Free Tubes

Figures 5-10 present the results for cantilevered tubes. Tube response characteristics depend on the flow velocity. At zero flow, the tube responds as a beam. As the flow velocity increases, tube damping values increase; the increase of damping is attributed to the Coriolis force. When the flow velocity is relatively high, the tube is critically damped; disturbances to the tube will not cause it to oscillate. However, when the flow velocity is further increased, damping becomes smaller and, eventually, the tube loses stability by flutter.

At low flow velocities, rms tube displacements are relatively small; the oscillations are caused by turbulent flow. Because of the increase in damping, tube responses do not increase in proportional to the flow velocity squared.

In the six tubes, only the tubes in Tests 1.1 and 1.2 become unstable; in the other four tubes, flow velocity is not high enough to cause flutter. As the flow velocity is increased to approach the critical value, relatively rapid increase results in tube-oscillation amplitude. In the high flow-velocity range, tube oscillations are predominantly associated with the second

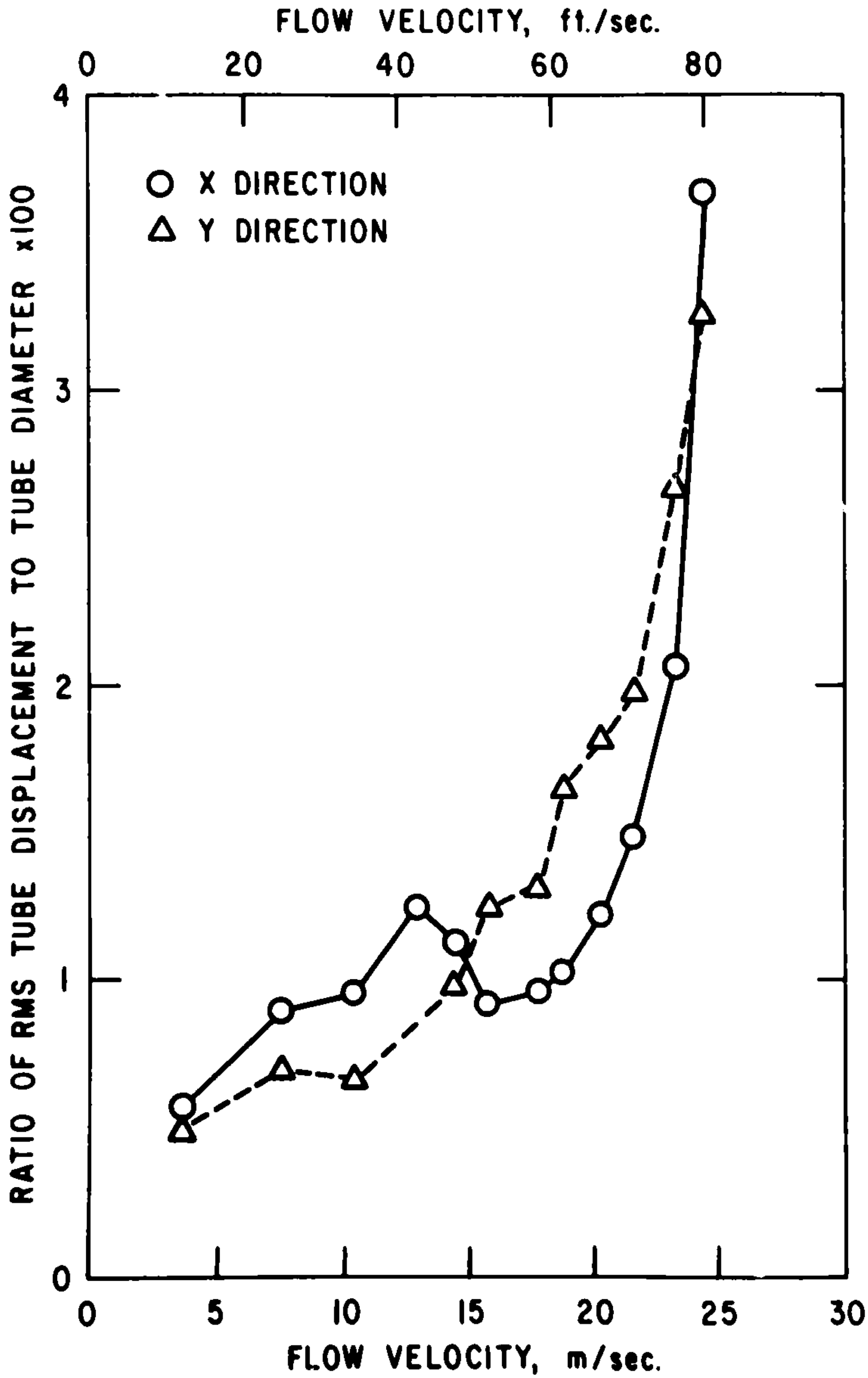

Fig. 5. RMS Tube Displacement as a Function of Flow Velocity for Test 1.1

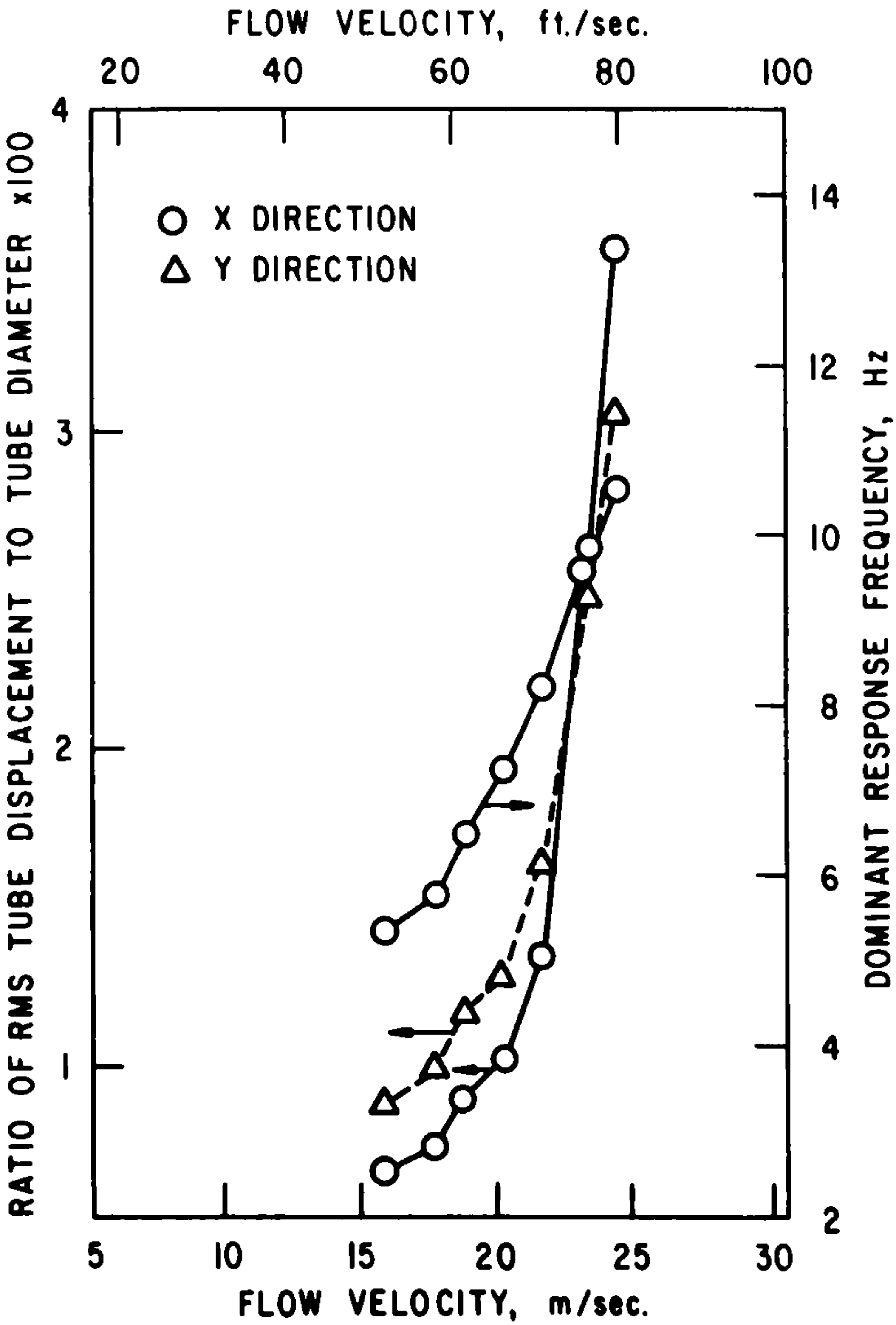

Fig. 6. RMS Tube Displacement and Frequency of the Second Mode for Test 1.1

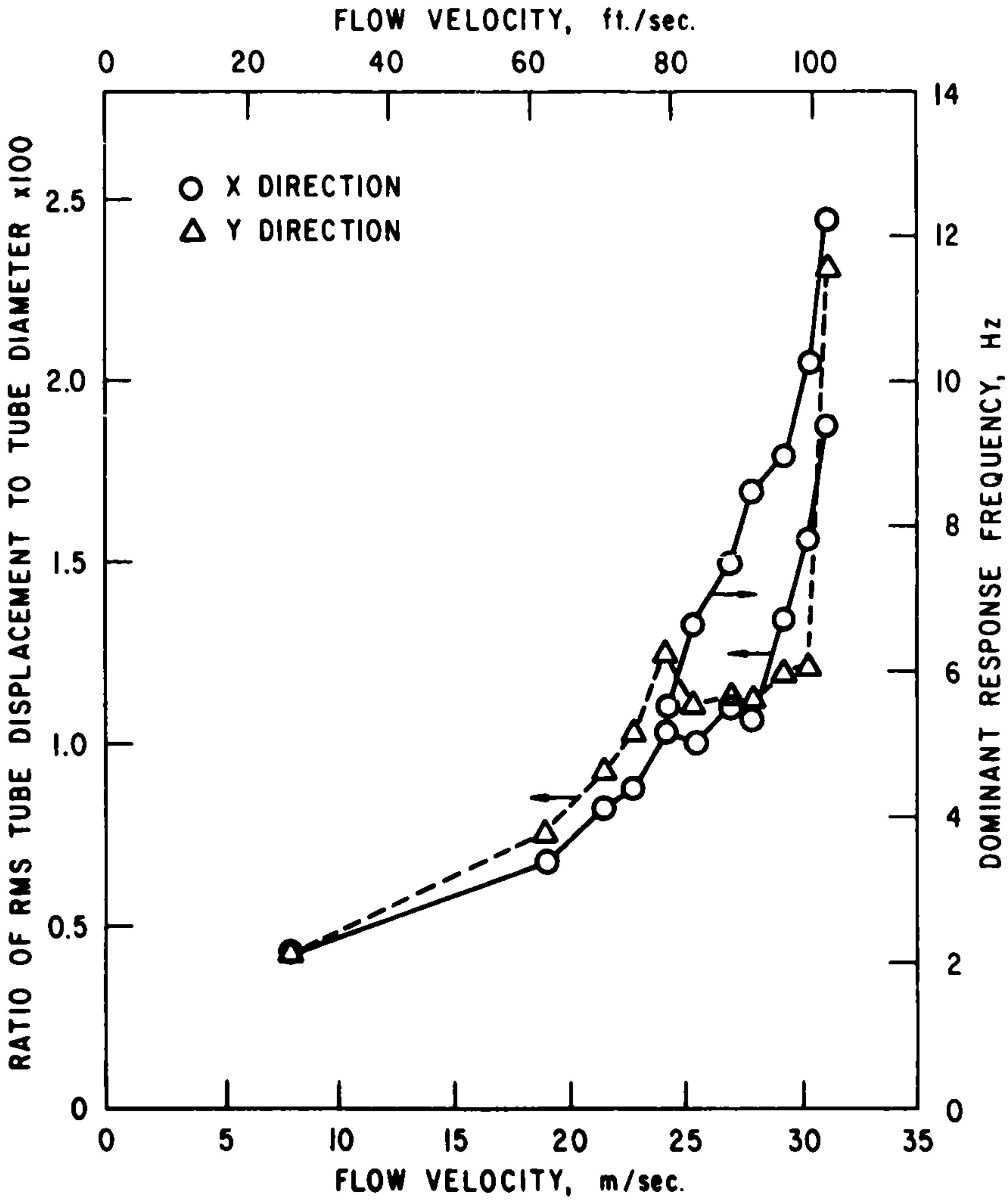

Fig. 7. RMS Tube Displacement and Dominant Response Frequency for Test 1.2

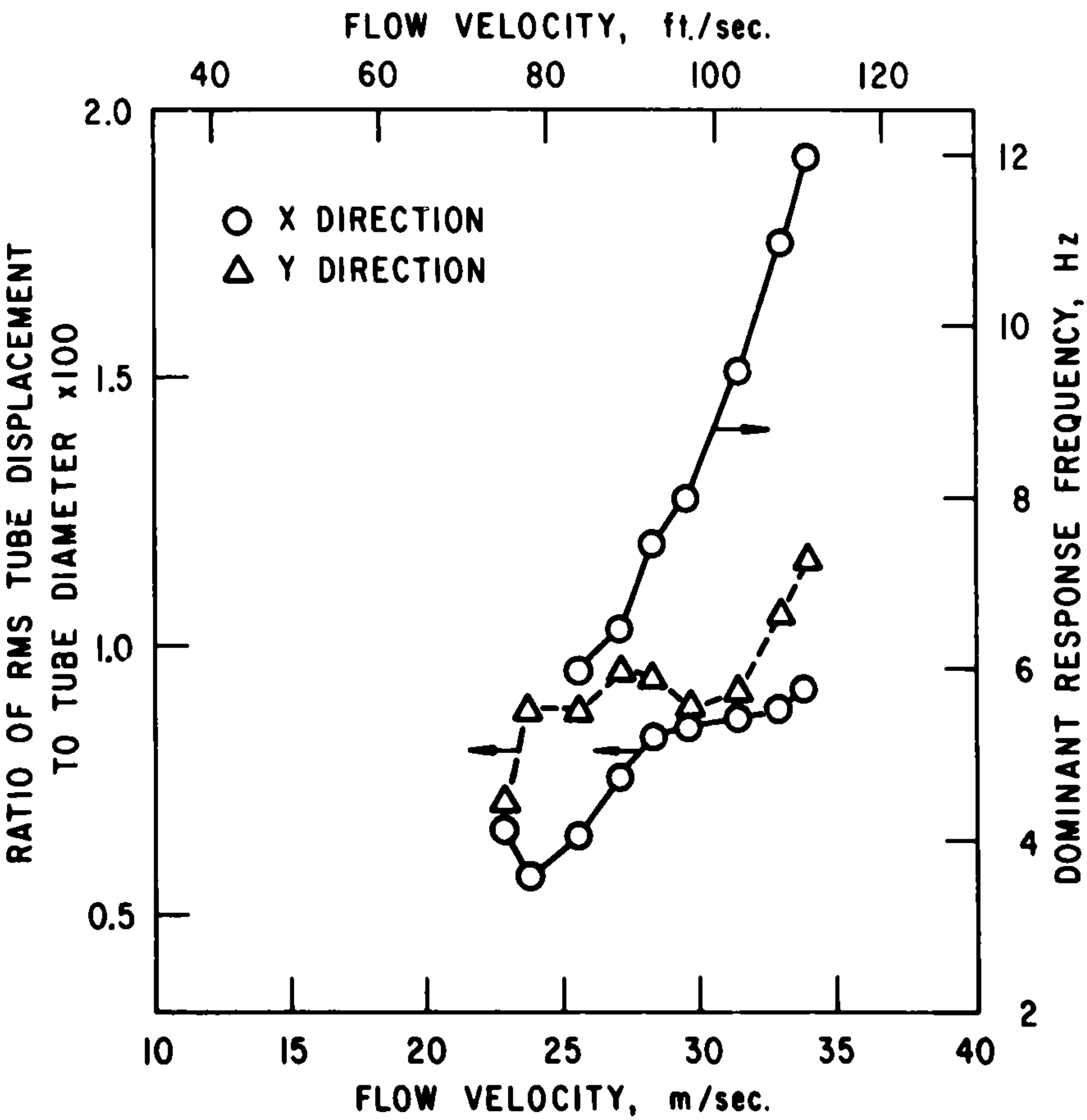

Fig. 8. RMS Tube Displacement and Dominant Frequency for Test 1.3

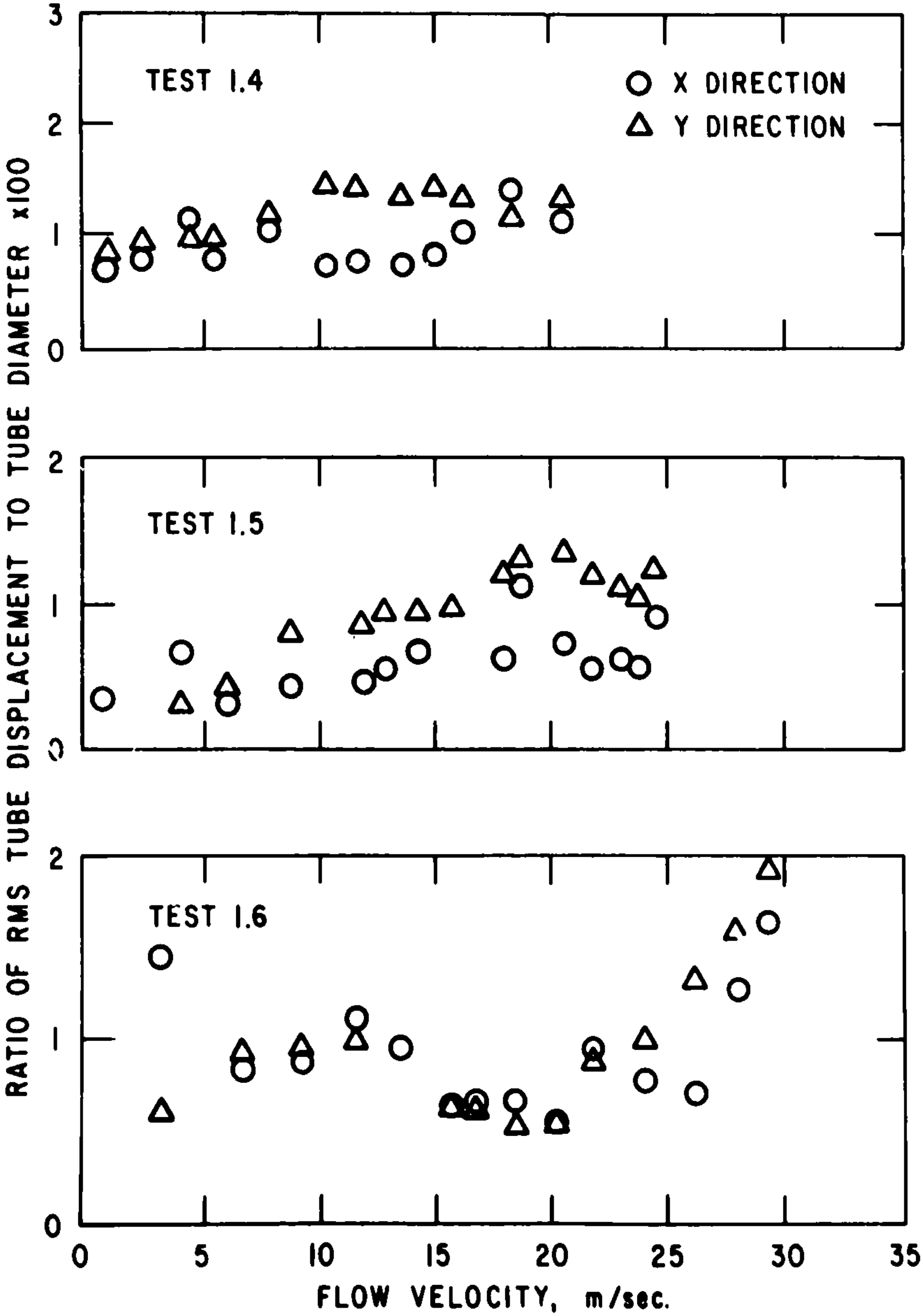

Fig. 9. RMS Tube Displacements for Tests 1.4, 1.5, and 1.6

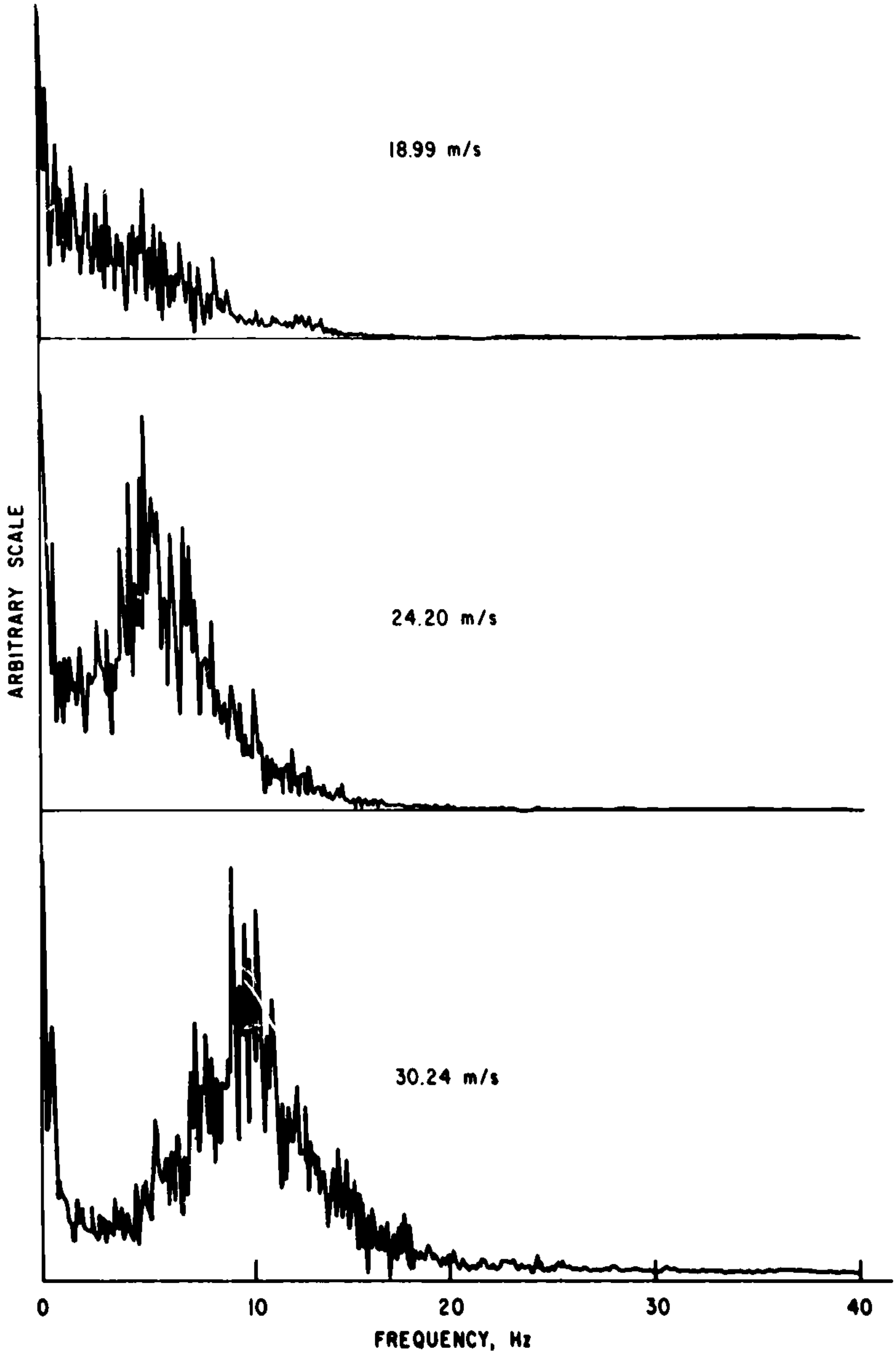

Fig. 10. Frequency Spectra of Tube Displacement for Test 1.2 at Several Flow Velocities

mode. This can be seen from Figs. 5 and 6. In Fig. 5, it gives the total tube displacement, while in Fig. 6, it gives the contribution from the second mode only. The sharp increase in tube-displacement response is attributed to the second mode.

Figure 10 shows typical frequency spectra at different flow velocities. At low flow rates, the frequency spectrum is broadly banded with no dominant frequency peaks. In this range of flow rates, tube oscillations are small. Most of the tube displacements given in Fig. 9 are in this region. With the increase in flow velocity, damping of the second mode decreases[4] and its natural frequency increases. At instability, the tube becomes unstable in the second mode and there is a sharp peak in the frequency spectra.

Table 2 gives the critical flow velocity and oscillation frequency, which can be determined from the tube displacement curves and frequency spectra, for Tests 1.1 and 1.2. The theory and experiment agree reasonably well. The theoretical values are based on the published results.[19,20]

The instability characteristics have been discussed in several publications.[4,6] For example, the "dragging motion" is one characteristic of such a system at instability. The observed phenomena are similar to the published results. However, the variation of rms displacements and the dominant response frequency appear not to have been reported before. Based on the results, a fixed-free tube appears to be fairly "rigid" in the subcritical flow velocity range. In this range of flow velocities, rms tube displacement is about 1% of tube diameter. Only when the flow velocity is close to its critical value, does the tube displacement increase more drastically.

B. Case 2: Tubes Fixed at the Upstream End and Supported by an Elastic Spring at the Downstream End

(1) Test 2.1. The detailed tube-response characteristics were not measured. The general characteristics are similar to those of a cantilevered tube. However, as the flow velocity increases, large displacement at the spring causes the tube to respond as a fixed-hinged tube. Therefore, no flutter was observed. According to the linear theory, the tube should lose stability by flutter if the spring responded linearly.[20]

(2) Test 2.2. Figures 11 and 12 show the tube static and rms displacements, and the dominant response frequencies as functions of flow velocity. A series of static deformation shapes is given in Fig. 13.

The static deformation increases with flow velocity; the deformation is caused by fluid centrifugal force. As the flow velocity is increased to a value close to the critical one, static deformation increases more rapidly. Note that there is a drastic change in static displacement

Table 2. Critical Flow Velocity for Case 1

Test	Fundamental Natural Frequency (Hz)		Critical Flow Velocity (m/s)		Oscillation Frequency at Instability (Hz)	
	Theory	Experiment	Theory	Experiment	Theory	Experiment
1.1	1.74	1.7	25.0	24.9	12.9	12.0
1.2	2.14	2.1	30.7	31.4	16.01	14.5

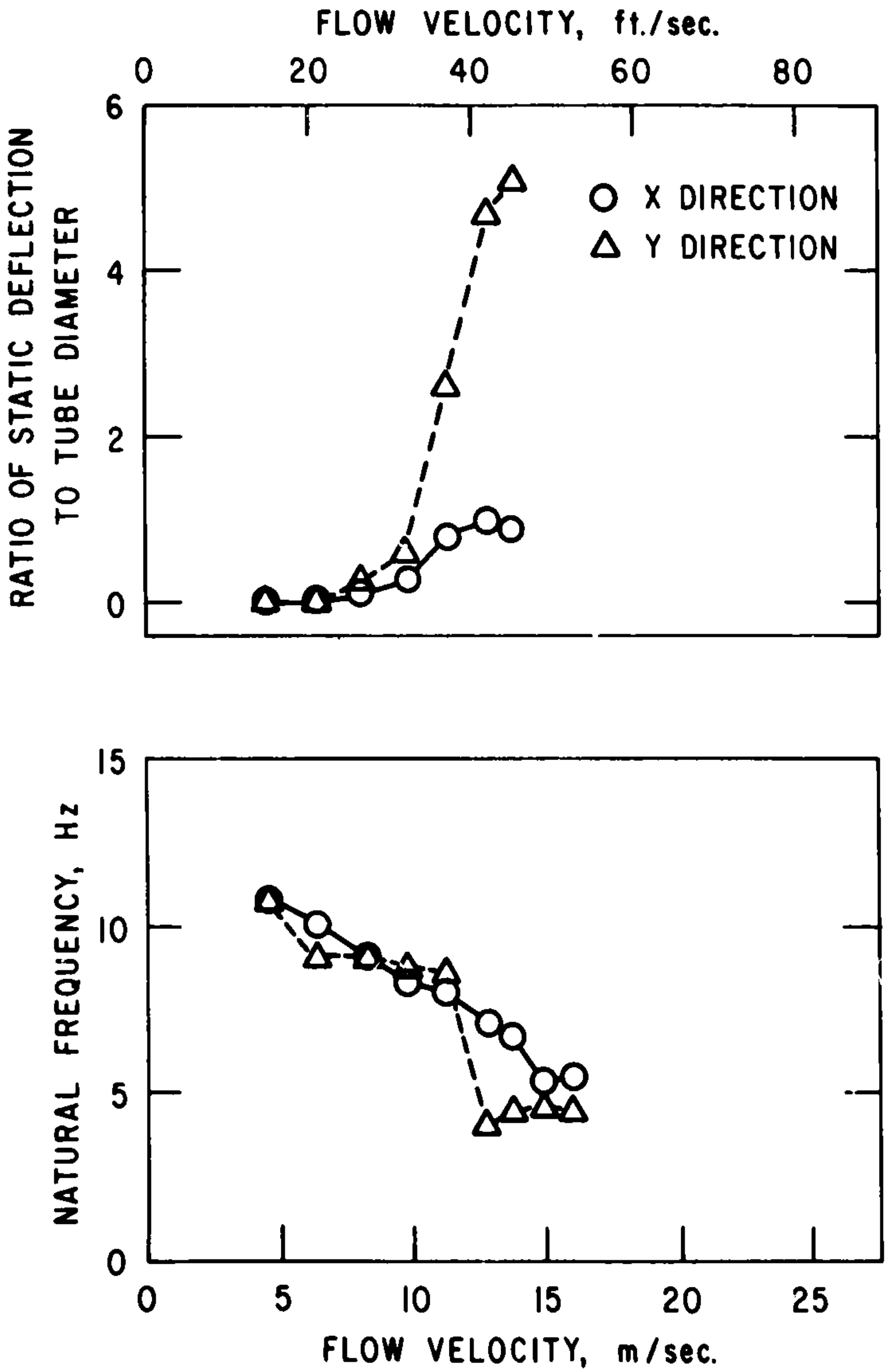

Fig. 11. Tube Static Displacement and the Natural Frequency of the Fundamental Mode for Test 2.2

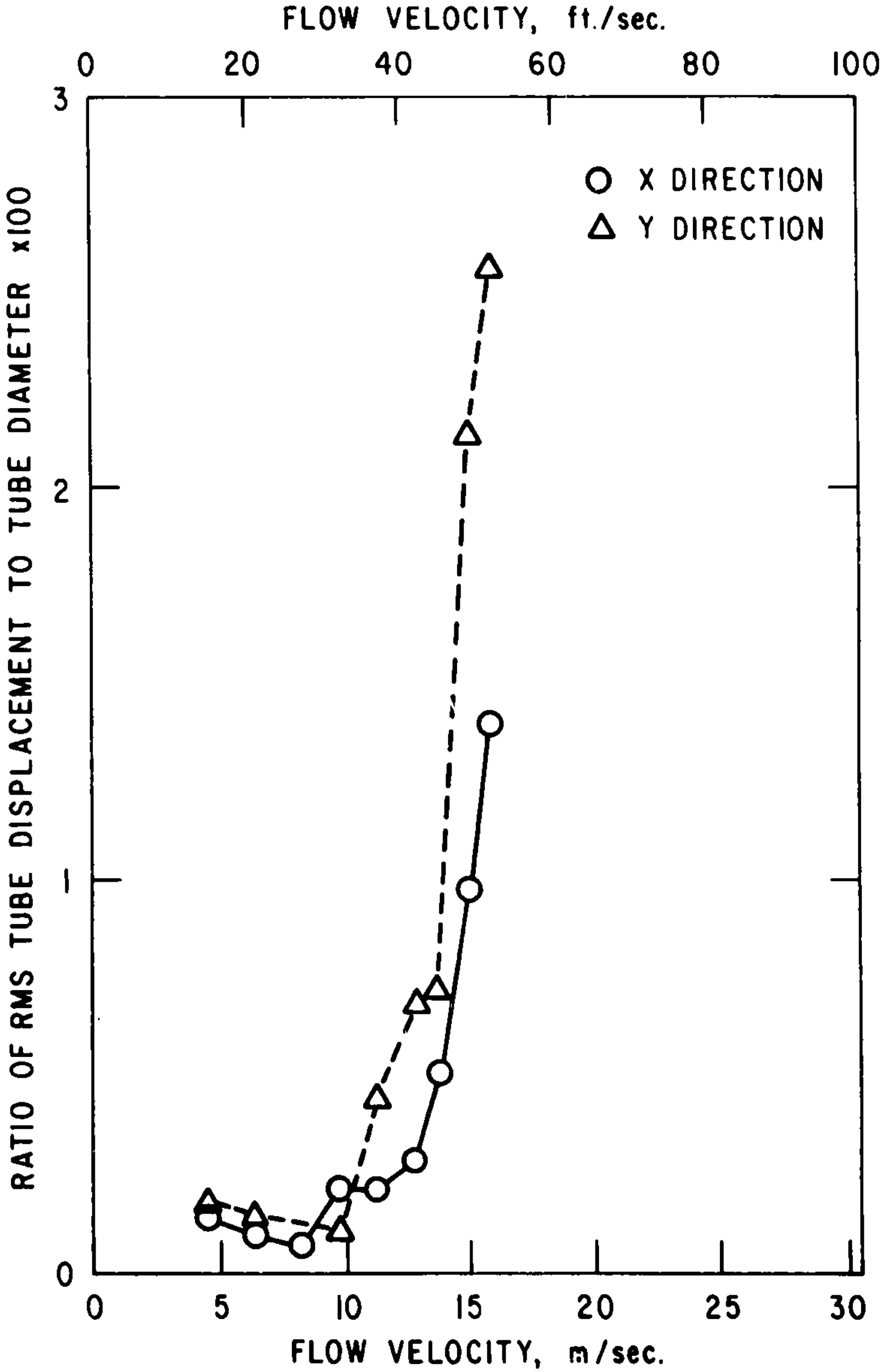

Fig. 12. RMS Tube Displacement for Test 2.2

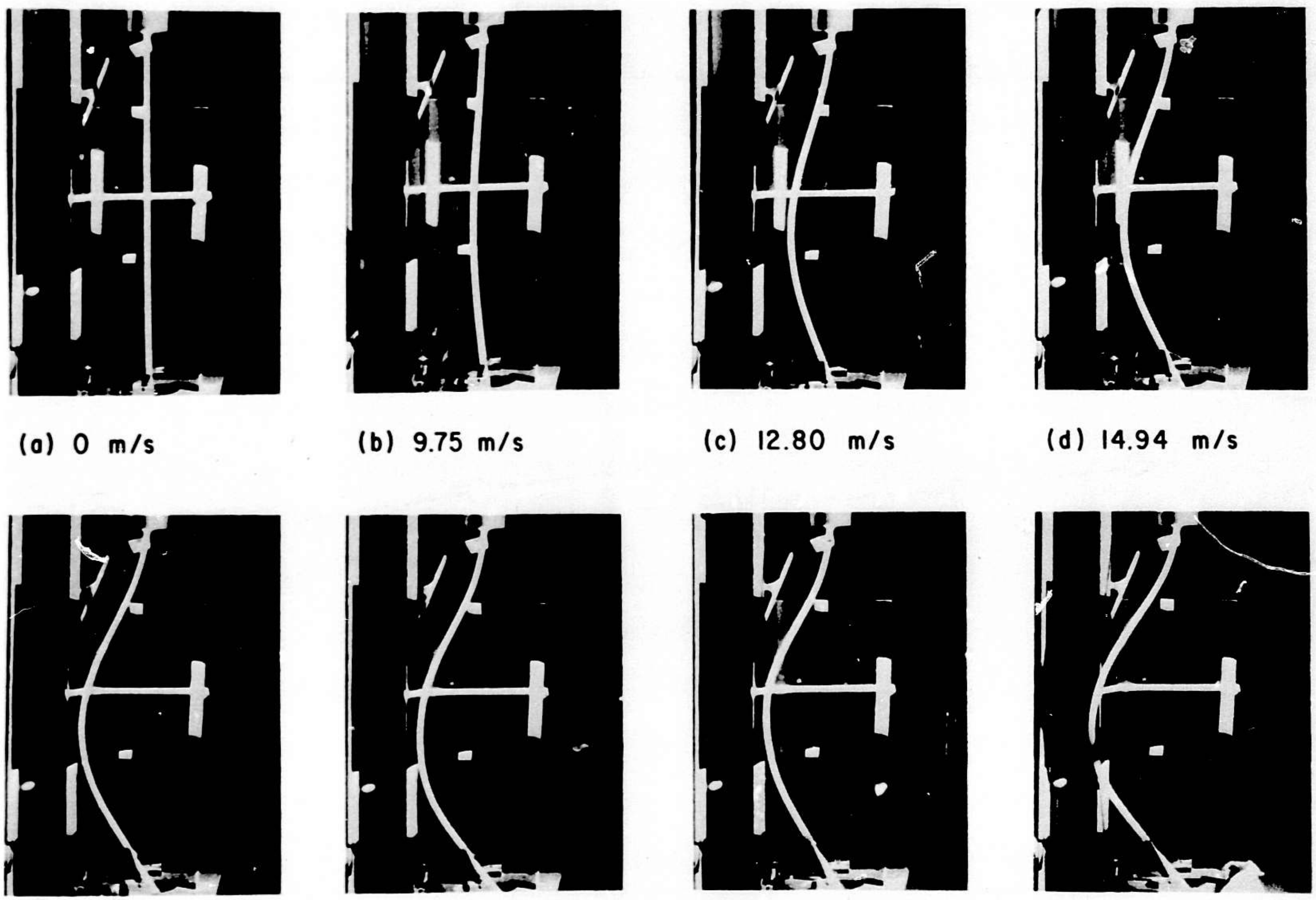

(a) 0 m/s (b) 9.75 m/s (c) 12.80 m/s (d) 14.94 m/s

(e) 17.07 m/s (f) 23.16 m/s (g) 24.69 m/s (h) 27.13 m/s

Fig. 13. Tube Static Deformation Shapes for Test 2.2. ANL Neg. No. 113-83-4.

and natural frequency at about 12 m/s (40 ft/sec); this is attributed to the imperfections in the experimental setup.

The dominant oscillation frequency is associated with the fundamental natural frequency, which decreases with flow velocity. Based on linear theory, the tube fundamental frequency will become zero and the tube will lose stability by buckling.[20] Because of the nonlinear effects associated with relatively large tube displacements and the nonlinear characteristics of the spring, the decrease in natural frequency is not as drastic as predicted.

The instability mechanisms depend on the spring constant.[20] Theoretically, the transition between the different instability mechanisms can be demonstrated by varying the spring constant. However, experimentally this type of support is difficult to simulate.

C. Case 3: A Fixed-Fixed Tube

Figures 14 and 15 show the tube displacement, natural frequency and modal damping ratio as functions of flow velocity.

The static displacement increases with flow velocity; the rate of increase is more significant at higher flow rates. Based on linear theory, the amplitude will increase continuously and the frequency will eventually become zero at the critical flow velocity. Accordingly, the critical flow velocity is calculated to be about 22.2 m/s (72.2 ft/sec). Because of the nonlinear effects, the instability is apparently limited as the static displacement is only about 0.5 tube diameter at 24 m/s (78.7 ft/sec).

The rms amplitudes increase with flow velocity at low flow rates. For a flow velocity larger than the critical value of 22.2 m/s (72.2 ft/sec) (linear theory), the rms tube displacement decreases. Again, this is attributed to the tension induced in the tube by large deformation; the two supports are not movable, and a large tensile force can be developed.

Modal damping ratio increases slightly with flow velocity. This is different from that in Case 1,[4] where damping increases rapidly with flow velocity because of the Coriolis force. For a fixed-fixed tube, the Coriolis force does not contribute damping; however, it can cause phase distortion such that classical normal modes do not exist. In addition, in this case, the damping value is much smaller than that of a fixed-free tube.

The results are in agreement with other tests.[10] When the tube is not allowed to move at both ends, the tension developed will suppress the effect of the fluid centrifugal force. The tube does not lose stability by divergence, contrary to prediction by linear theory.

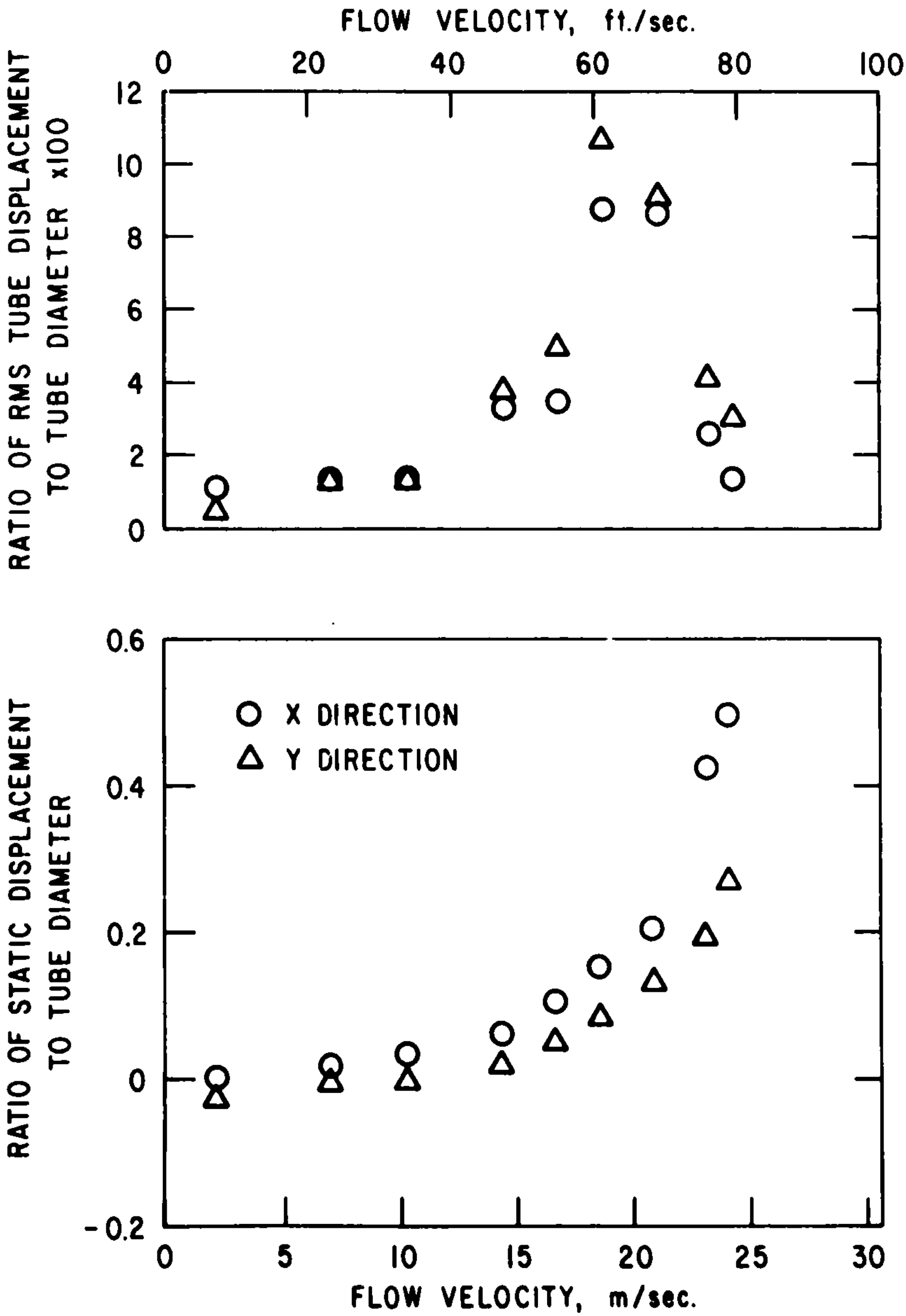

Fig. 14. Tube Displacement Components for Test 3

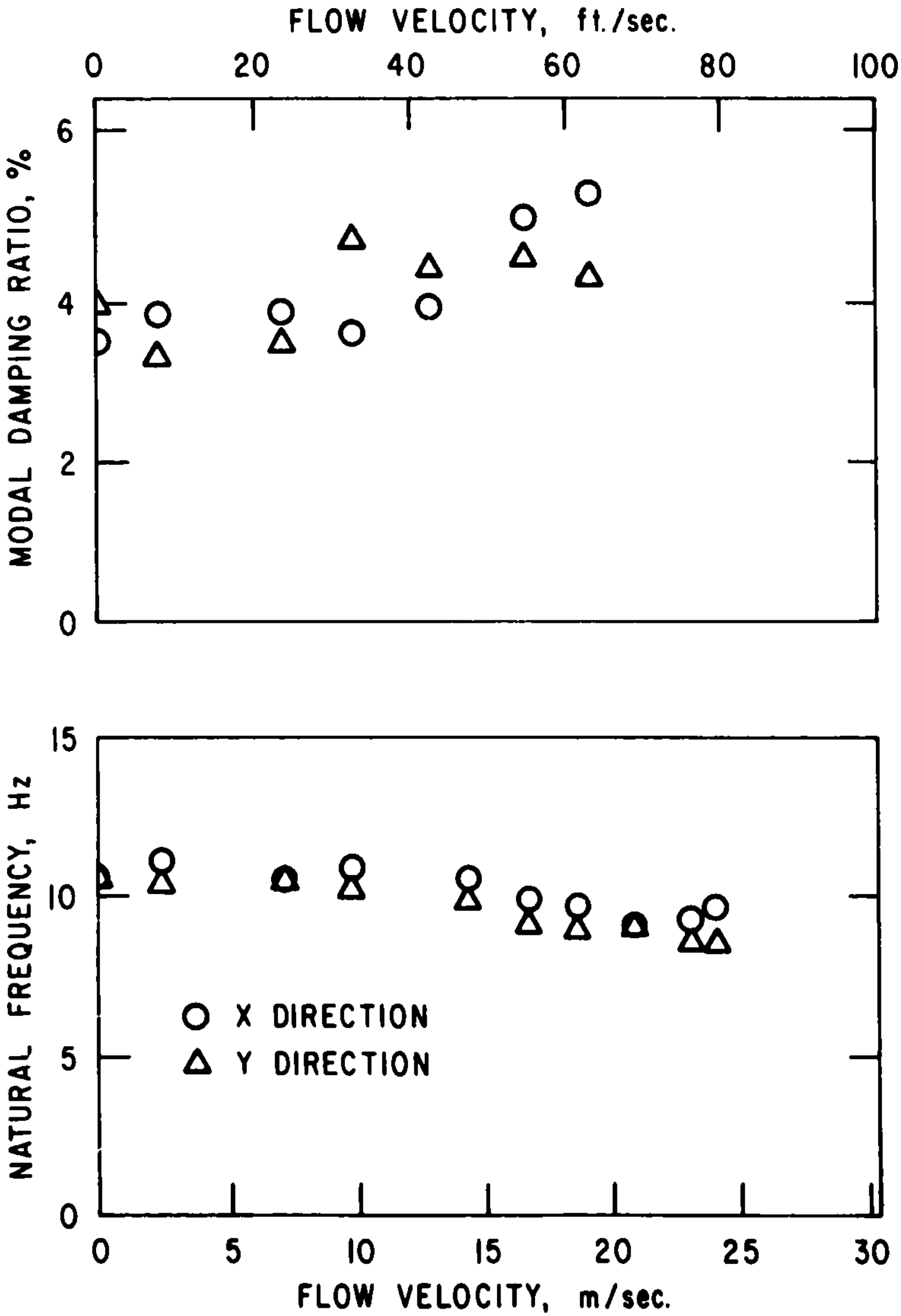

Fig. 15. Tube Natural Frequency and Modal Damping Ratio for Test 3

D. Case 4: Tubes Fixed at the Upstream End and a Knife-edge Support Movable along the Tube

The tube-response characteristics depend on the location of the hinged support. For small values of ℓ/L (see Fig. 3), the behavior of the tube is basically similar to that of a fixed-free tube. For large values of ℓ/L, the tube responds as a fixed-hinged tube. A fixed-free tube is known to lose stability by flutter and a fixed-hinged tube is known to become unstable by divergence. Therefore, at a certain value of ℓ/L, the instability will switch from one mechanism to the other.

Figures 16-18 show the rms tube displacement, the dominant response frequency, and the modal damping ratio for small values of ℓ/L. The rms displacement increases with flow velocity, but it is not a monotonically increasing function of flow velocity. For example, for $\ell/L = 0.194$ and 0.266, in a certain range of flow velocity, the rms displacement decreases with flow velocity. The dominant response frequency increases with flow velocity and ℓ/L (see Fig. 18). The trend is similar to that of a fixed-free tube.

At low flow velocity, the modal damping value is very large. When the flow velocity is increased to a value near the flutter flow velocity, the damping value decreases with flow velocity (see Fig. 17). When the modal damping value becomes zero, the tube loses stability by flutter.

Figure 19 shows the frequency spectra of tube displacement for different flow velocities. At low flow velocities, the frequency spectra are more broad banded. At instability ($U \sim 23.5$ ft/sec), the frequency spectrum contains a sharp peak only.

Figure 20 shows the static tube displacement for large values of ℓ/L. The rms tube displacement and response frequency are not measured for this case. The static displacement increases with flow velocity; this is attributed to the fluid centrifugal force. For large values of ℓ/L, the system is less stable. For these values of ℓ/L, the tube loses stability by divergence.

The critical flow velocity for Test 4.1 is given in Fig. 21. For small values of ℓ/L, the instability is the flutter type. The flutter flow velocity can be determined from the following data: (1) rms tube displacement as a function of flow velocity--a drastic increase in rms displacement at a certain flow velocity; (2) frequency spectra--a sharp frequency peak; and (3) modal damping ratio--a zero damping value. For large values of ℓ/L, the divergence flow velocity is determined from the static displacement curve. The transition of the two instability mechanisms occurs at ℓ/L equal to about 0.3. Note that the critical flow velocity for flutter increases with ℓ/L, while that for divergence decreases with ℓ/L.

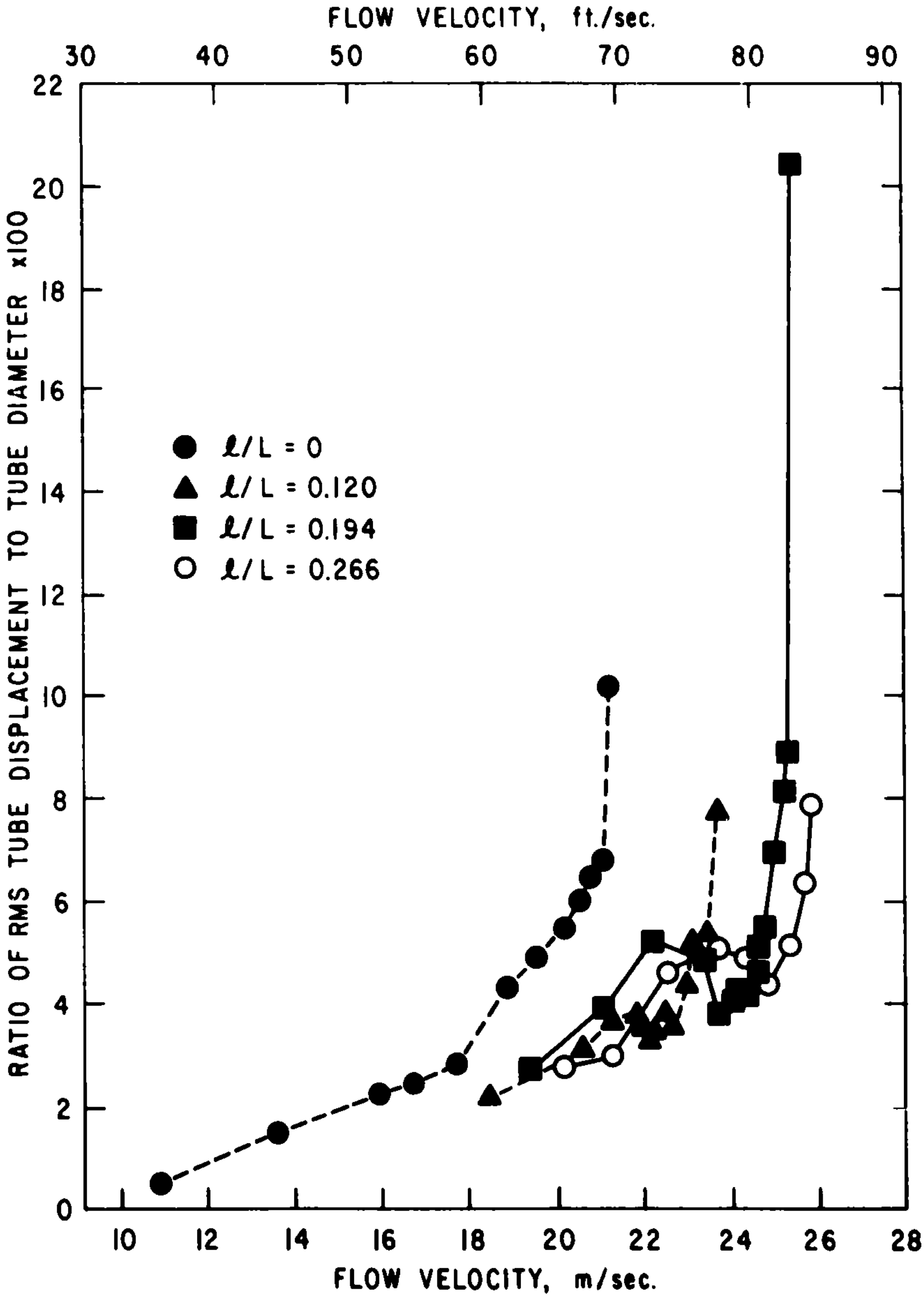

Fig. 16. RMS Tube Displacements as a Function of Flow Velocity for Test 4.1

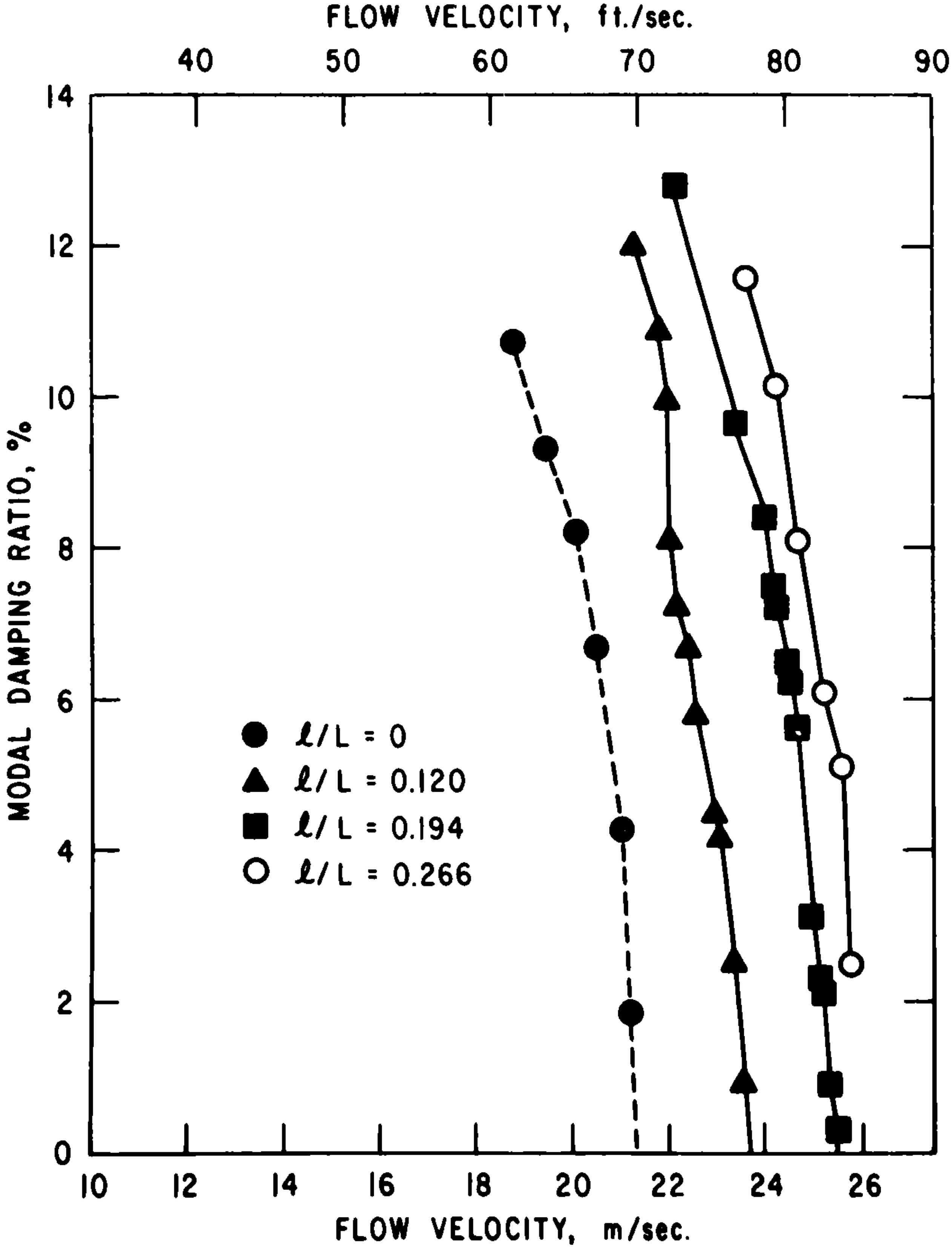

Fig. 17. Modal Damping Ratio as a Function of Flow Velocity for Test 4.1

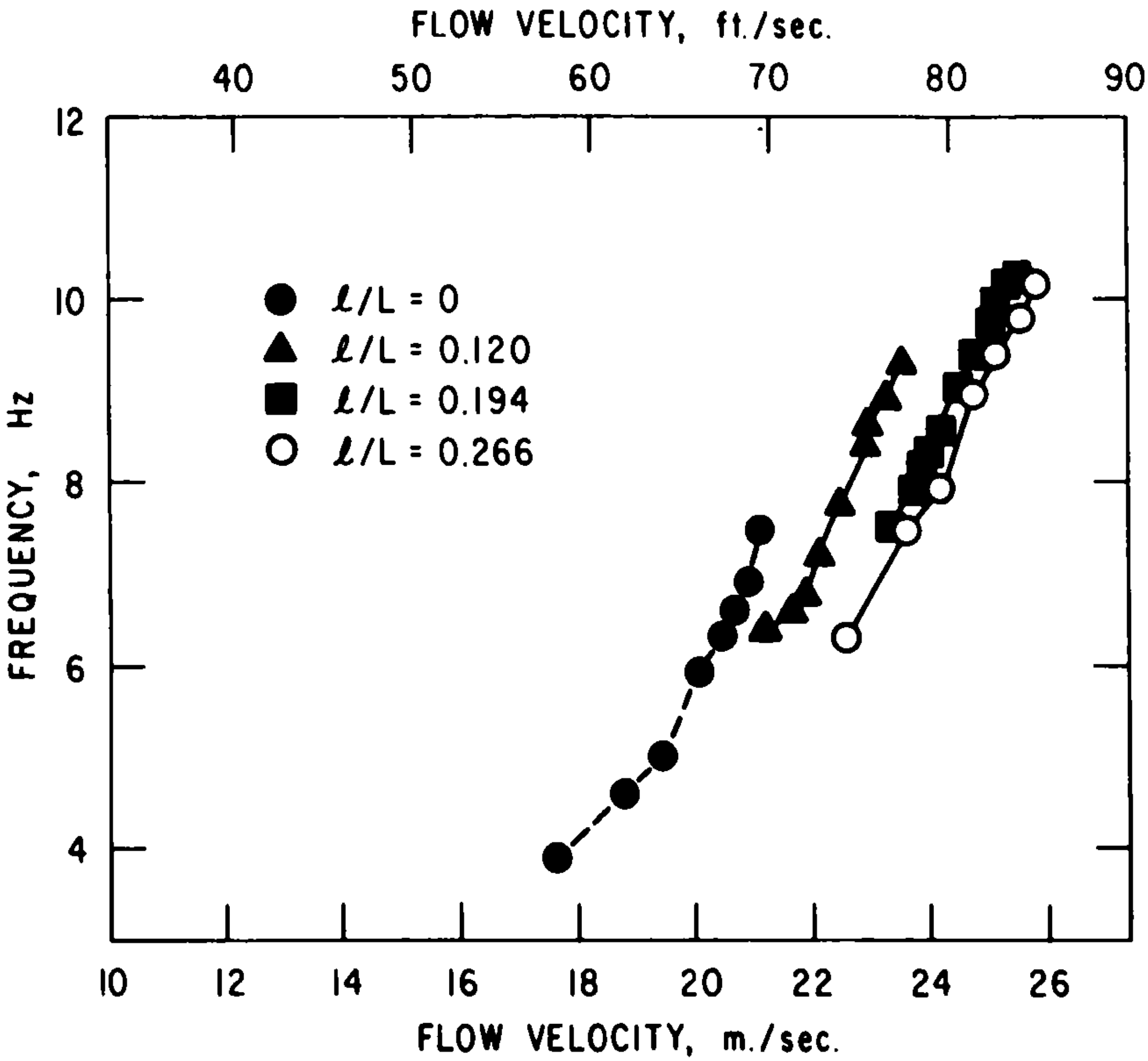

Fig. 18. Dominant Response Frequency for Test 4.1

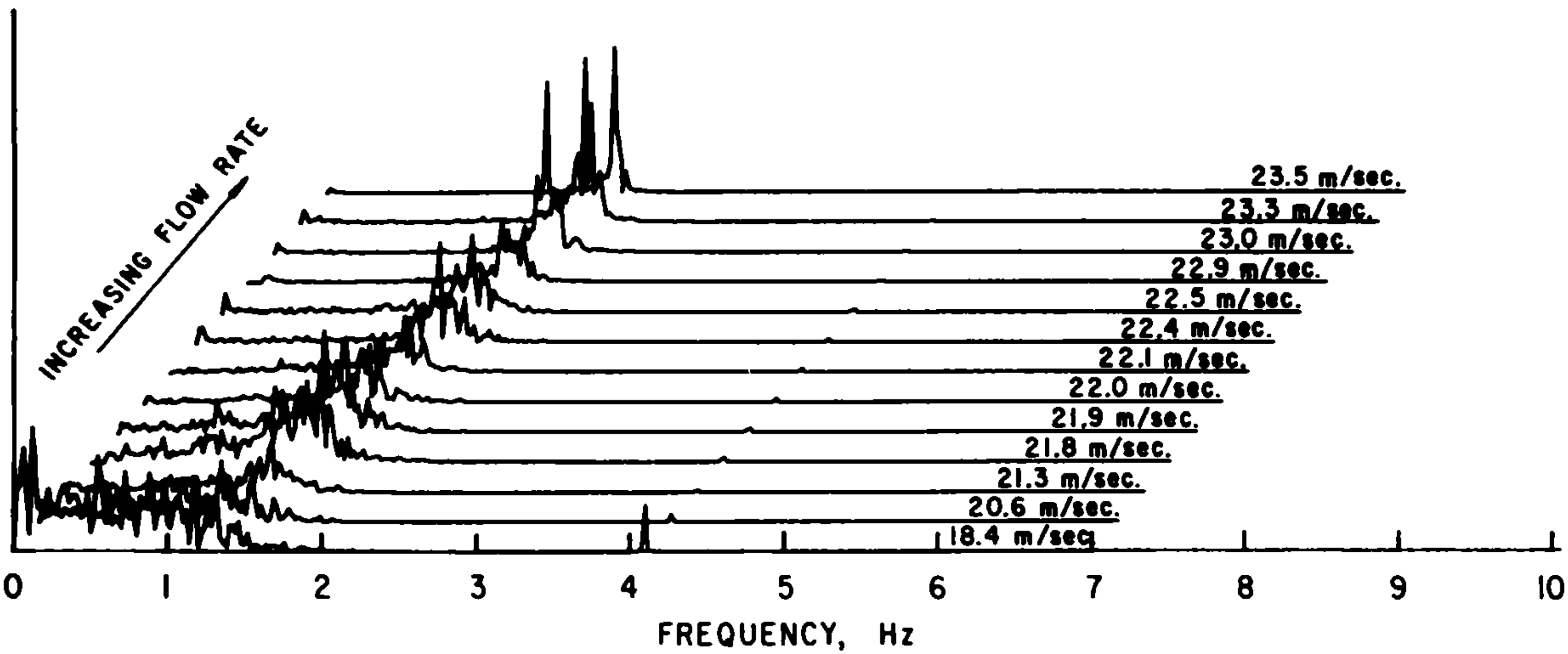

Fig. 19. Frequency Spectra of Tube Displacement at Various Flow Velocities for Test 4.1 with $\ell/L = 0.12$

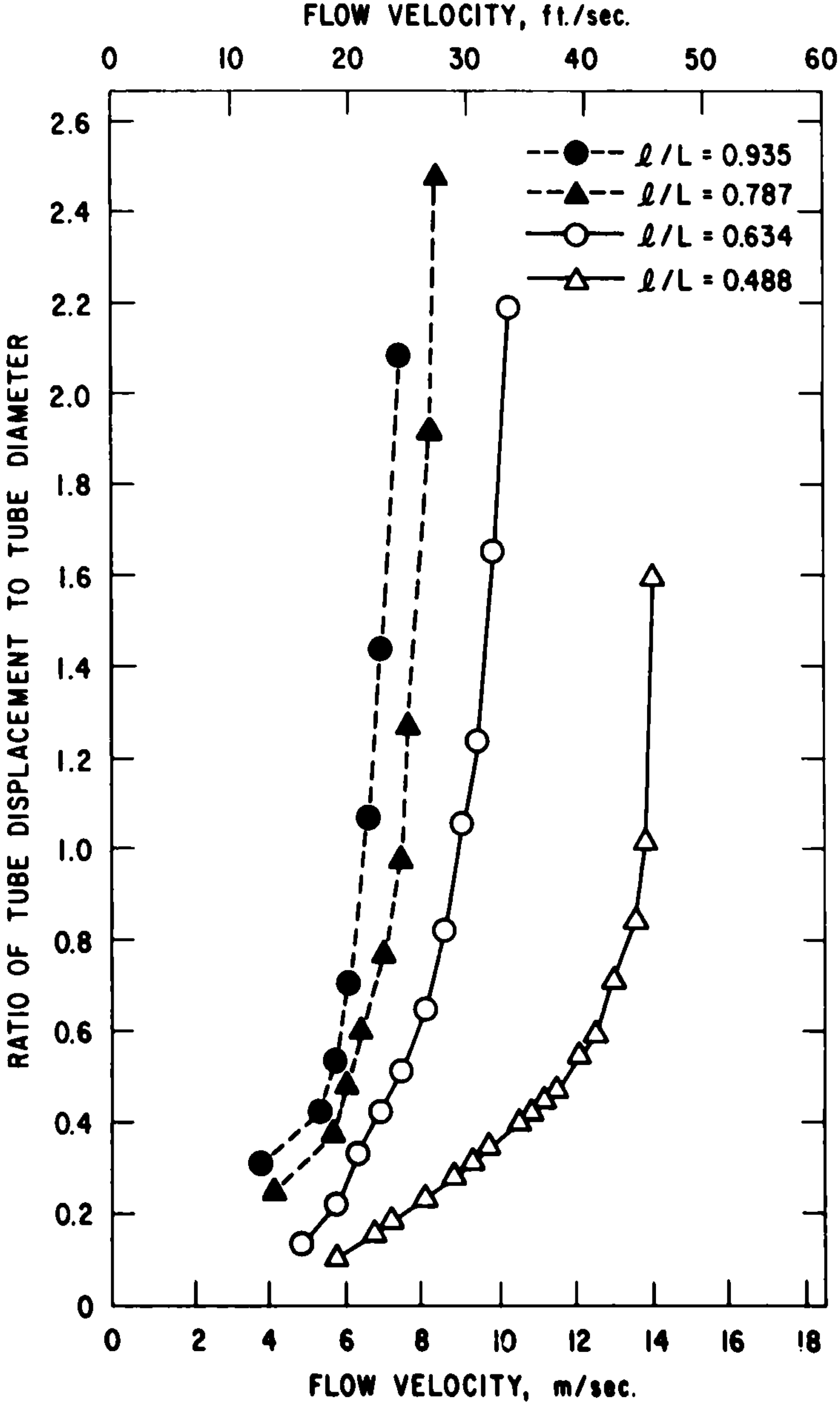

Fig. 20. Static Tube Displacements as a Function of Flow Velocity for Test 4.1

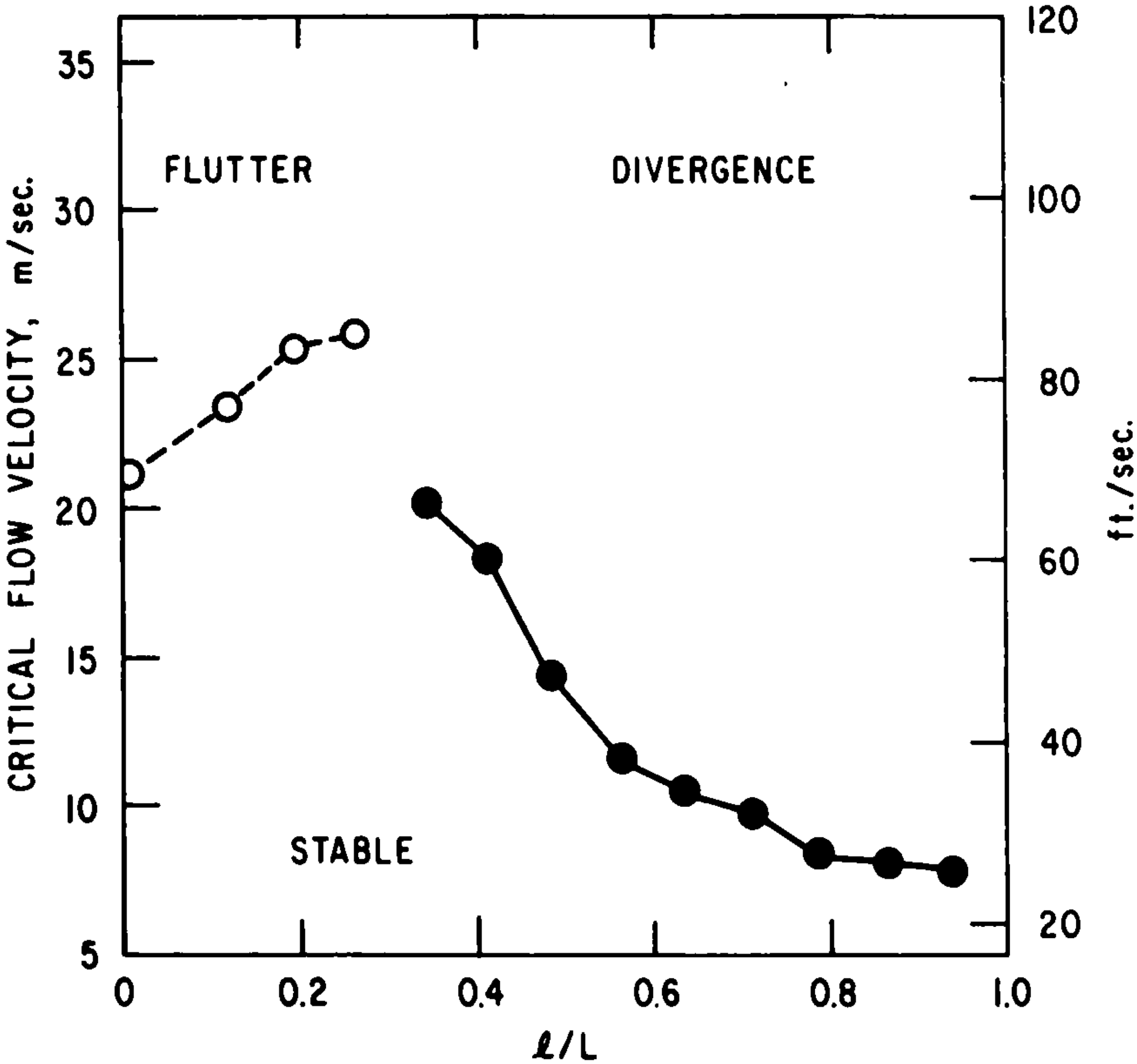

Fig. 21. Critical Flow Velocity for Test 4.1

Similar results are obtained for Test 4.2. While the detailed results are not included in this report, the stability diagram is shown in Fig. 22. Again, there is a transition between different mechanisms of instability at a certain value of ℓ/L.

In Tests 4.1 and 4.2, the intersection point of divergence and flutter was not obtainable in experiment because of the limitation of the water loop. Practically, it would be interesting to observe the tube response at the transition value of ℓ/L.

The flutter flow velocity for $\ell/L = 0$ agrees with the theoretical value reasonably well; the critical flow velocities based on linear theory are 22.8 m/s (74.8 ft/sec) and 20.7 m/s (67.9 ft/sec) for Tests 4.1 and 4.2 respectively. However, the divergence flow velocity calculated from the linear theory is much larger than the data; this is attributed to the fact that the fluid pressure is not accounted for in the calculation.

E. Case 5: A Cantilevered Tube with a Concentrated Mass Attached at the Free End

(1) Test 5.1. Figures 23-25 present the results for Test 5.1. The natural frequency for the fundamental mode is 0.51 Hz. The contribution of the first mode to tube response is small. The dominant frequency at higher flow rate is the second mode frequency which decreases with increasing flow velocity. This is contrary to the dynamic behavior displayed in Cases 1 and 4.

The modal damping ratio of the second mode first increases with the flow velocity and then decreases with the flow. When the flow velocity is close to the critical value, it decreases very drastically. At the same time, the tube displacement increases drastically.

The critical flow velocity of the system is 18.8 m/s (61.7 ft/sec). The oscillation frequency at instability is 2.7 Hz. The frequency is fairly low. Consequently, it takes a long time for the tube to build up to a large displacement. The curves illustrating "build-up" at four different flow velocities above the critical values are given in Fig. 25. At 19.0 m/s (62.3 ft/sec), it takes about 30 sec to reach a large displacement. However, at 20.2 m/s (66.3 ft/sec), it takes only about 6 sec.

Among all the different tests, Test 5.1 is the one test configuration that responds in an easily controllable manner and with characteristics that can be observed visually without difficulty. Therefore, for stability control, a system similar to that of Case 5 is chosen for further study.

(2) Test 5.2. The tube for Test 5.2 is basically the same as that for Test 5.1. The only difference is that the attached weight is a little heavier, and the length of the attached weight is a little longer.

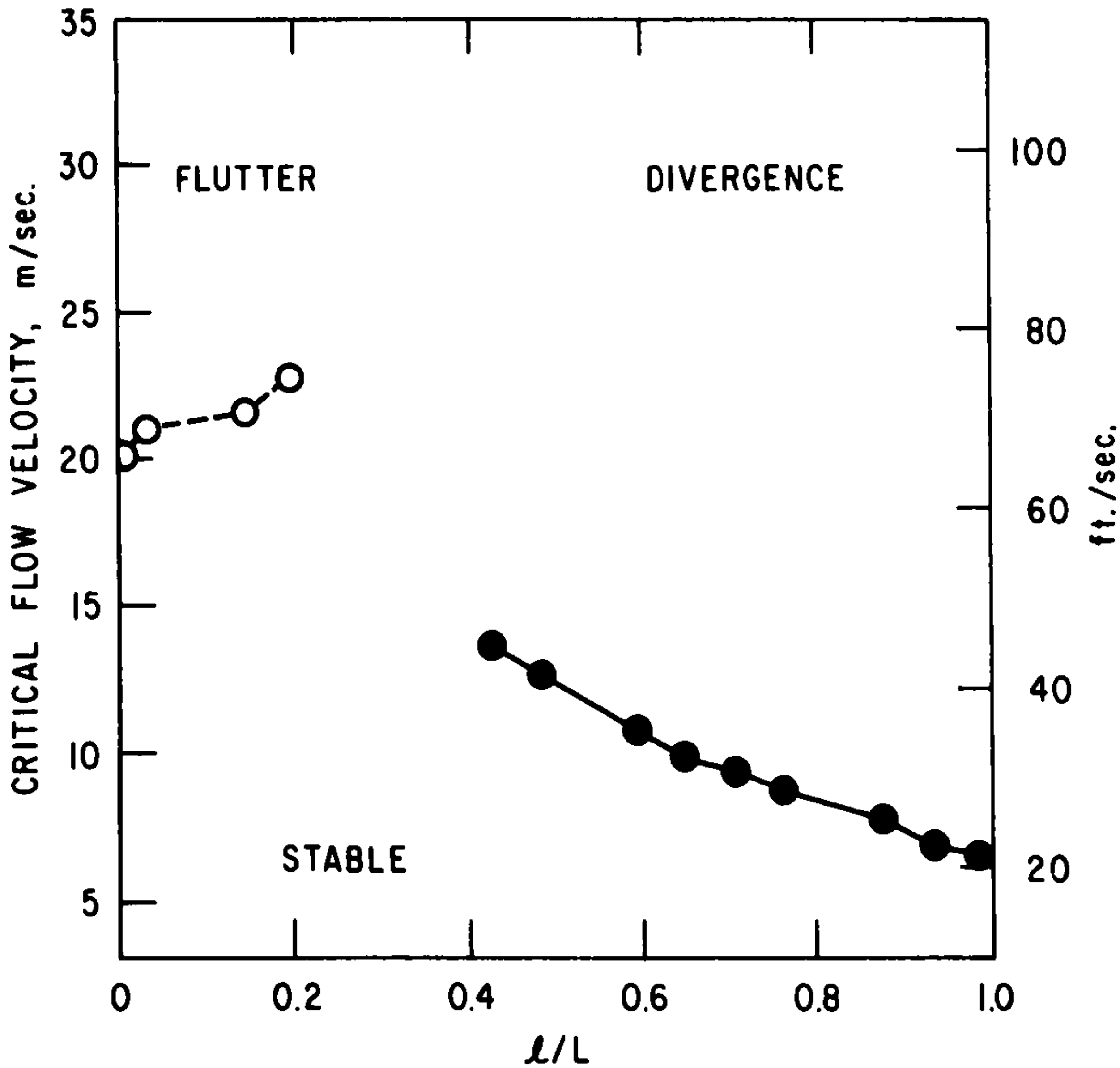

Fig. 22. Critical Flow Velocity for Test 4.2

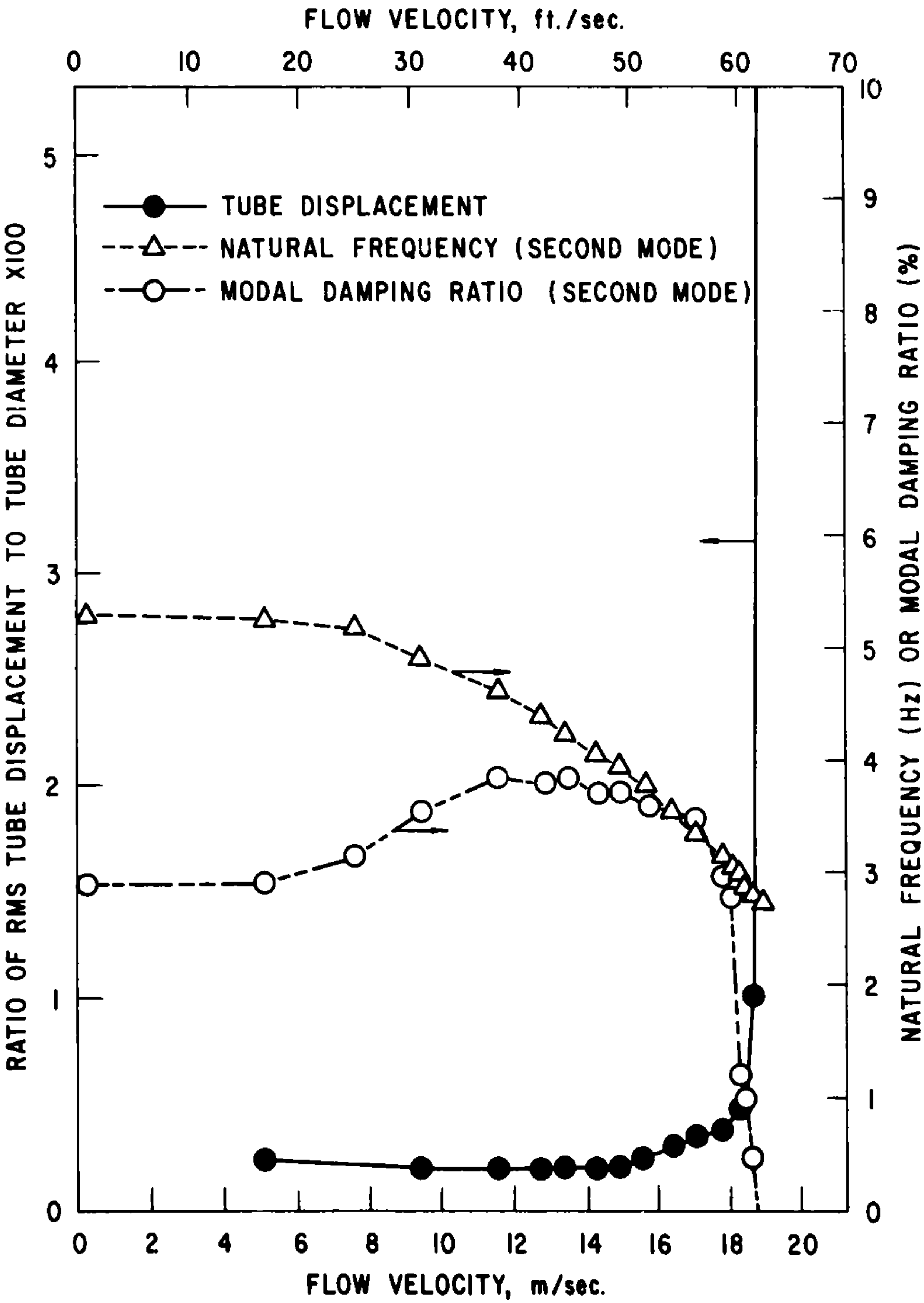

Fig. 23. RMS Tube Displacement, Natural Frequency, and Modal Damping Ratio of the Second Mode for Test 5.1

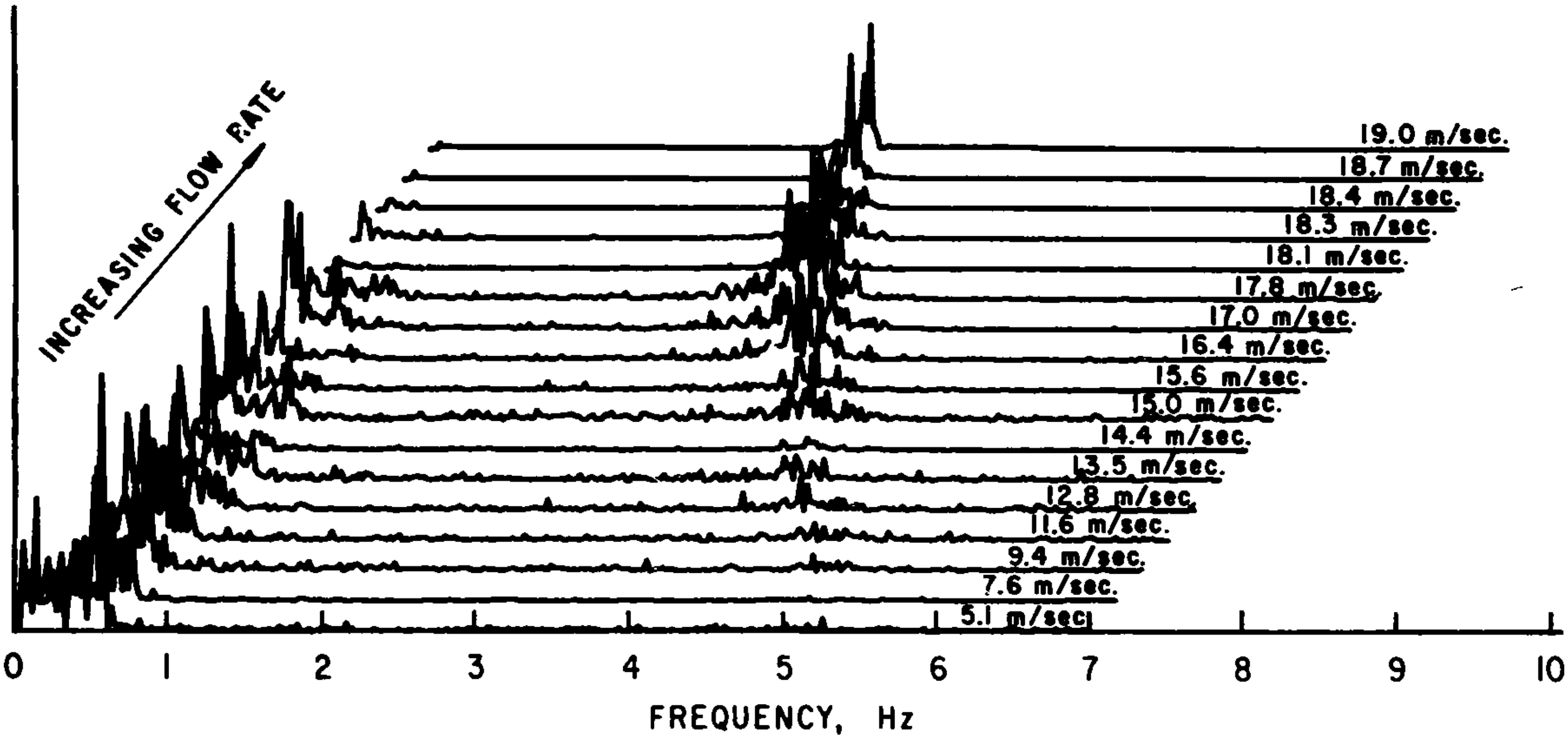

Fig. 24. Frequency Spectra of Tube Displacement at Various Flow Velocities for Test 5.1

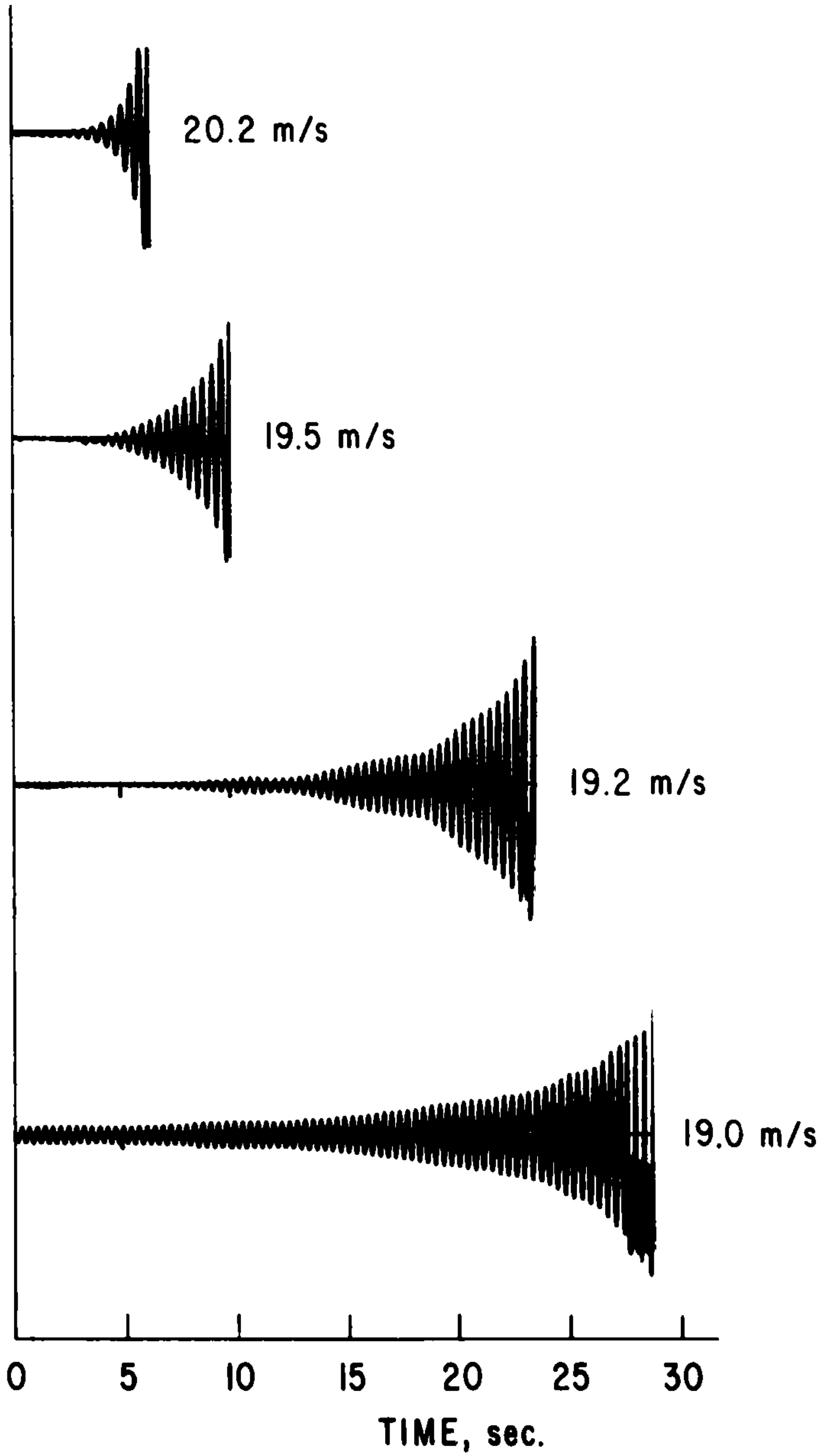

Fig. 25. Time History of Tube Oscillations at Various Flow Velocities for Test 5.1

Figure 26 shows the natural frequency and modal damping ratio of the fundamental mode as a function of flow velocity; these are obtained by impact excitation of the tube. The fundamental natural frequency is practically constant for flow velocities up to 12 m/s (39.4 ft/sec), and the damping can be observed to increase approximately linearly with the flow velocity. However, for higher flow velocities, the damping is large and the fundamental mode is difficult to excite.

Figure 27 shows the natural frequency and modal damping ratio of the second mode. Two methods are used: swept sine excitation and log decrement. The results are similar to those given for Test 5.1. Note that the tube loses stability by flutter in the second mode. In the high flow-velocity range, the frequency and damping values obtained by the two methods are not identical. This is attributed to the interaction of the flow and excitation force.

Figures 28 and 29 show the tube displacements for various types of excitations. In Fig. 28, the mechanical excitation is a sinusoidal force with a fixed frequency and amplitude; this type of excitation is referred to as an external control force. In Fig. 29, the excitation force is proportional to the measured tube displacement; this is referred to as a feedback control force. For comparison, the displacement due to flow only is also presented in Figs. 28 and 29.

The external control force appears to have little effect on the critical flow velocity. At low flow rate, the interaction of flow and control force is insignificant. At the flow rate close to the critical value, the interaction becomes larger. For example, the external control force at 2 or 8 Hz tends to stabilize the tube. However, the effect on the critical flow velocity is insignificant.

For feedback control, the effect on the critical flow velocity is much more important. The positive control force, which is in phase with the tube displacement, destabilizes the tube. The negative control force, which is out of phase with the tube displacement, stabilizes the tube.

The tube with feedback control force depends on the characteristics of the feedback system. In Test 5.2, the feedback control force is either in phase or out of phase with respect to the tube displacement. The tube and feedback loop are basically a nonlinear system. However, for small displacements, the response of the tube may be characterized as a linear system for most of the flow region except close to the critical value. Figure 30 shows the equivalent modal damping with negative and positive control forces. It is seen that the tube with positive control force possesses smaller values of damping.

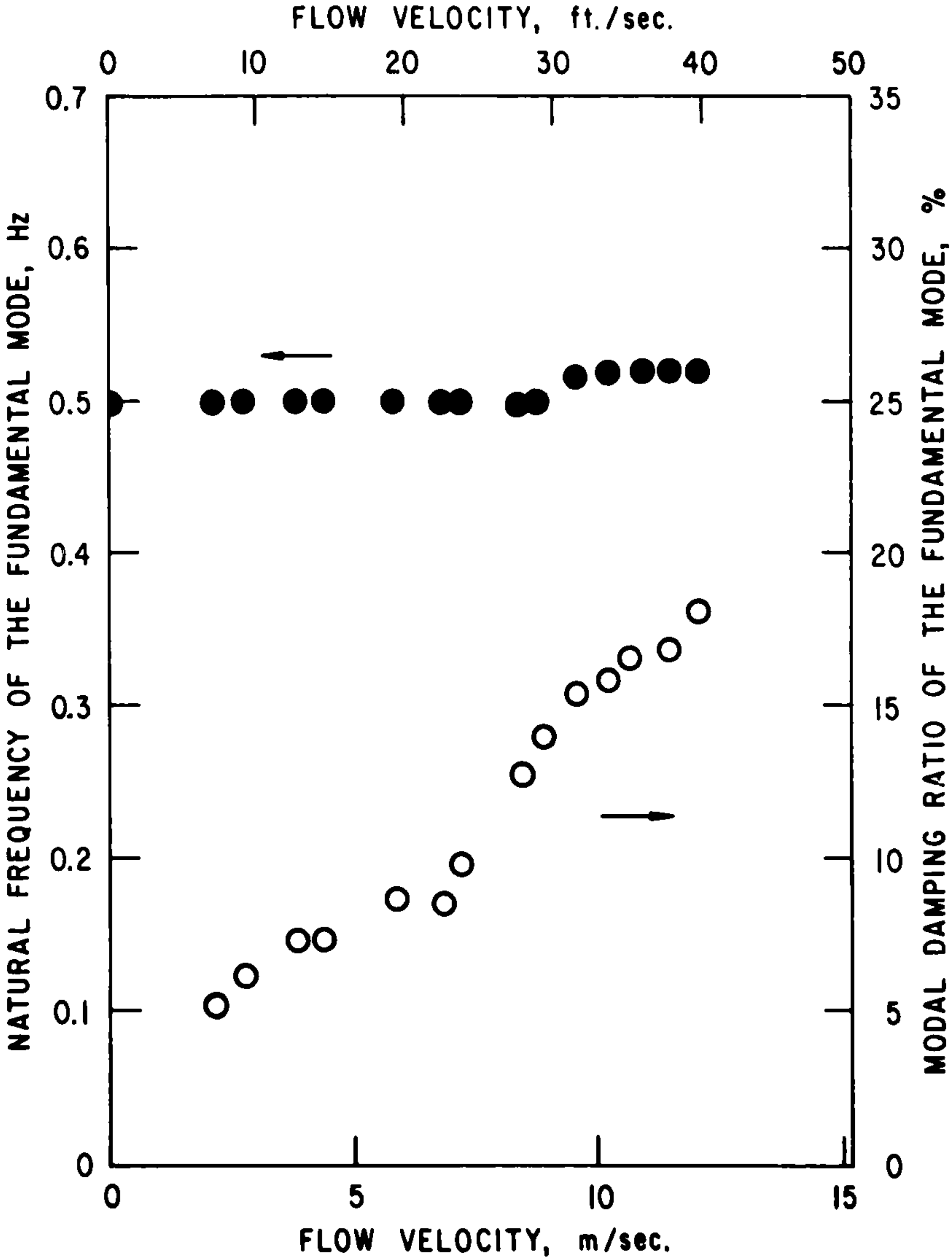

Fig. 26. Natural Frequency and Modal Damping Ratio of the Fundamental Mode for Test 5.2

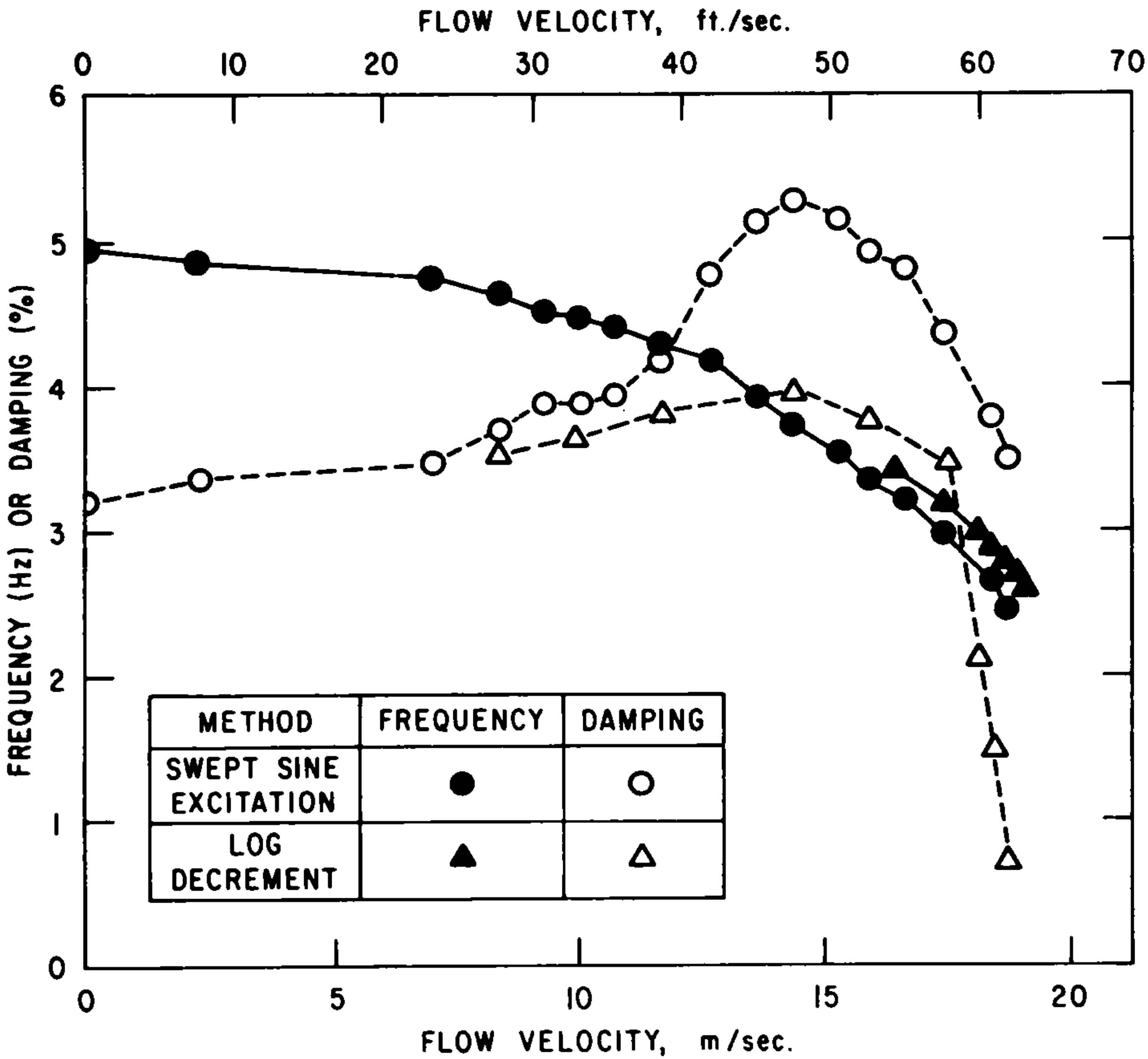

Fig. 27. Natural Frequency and Modal Damping Ratio of the Second Mode for Test 5.2

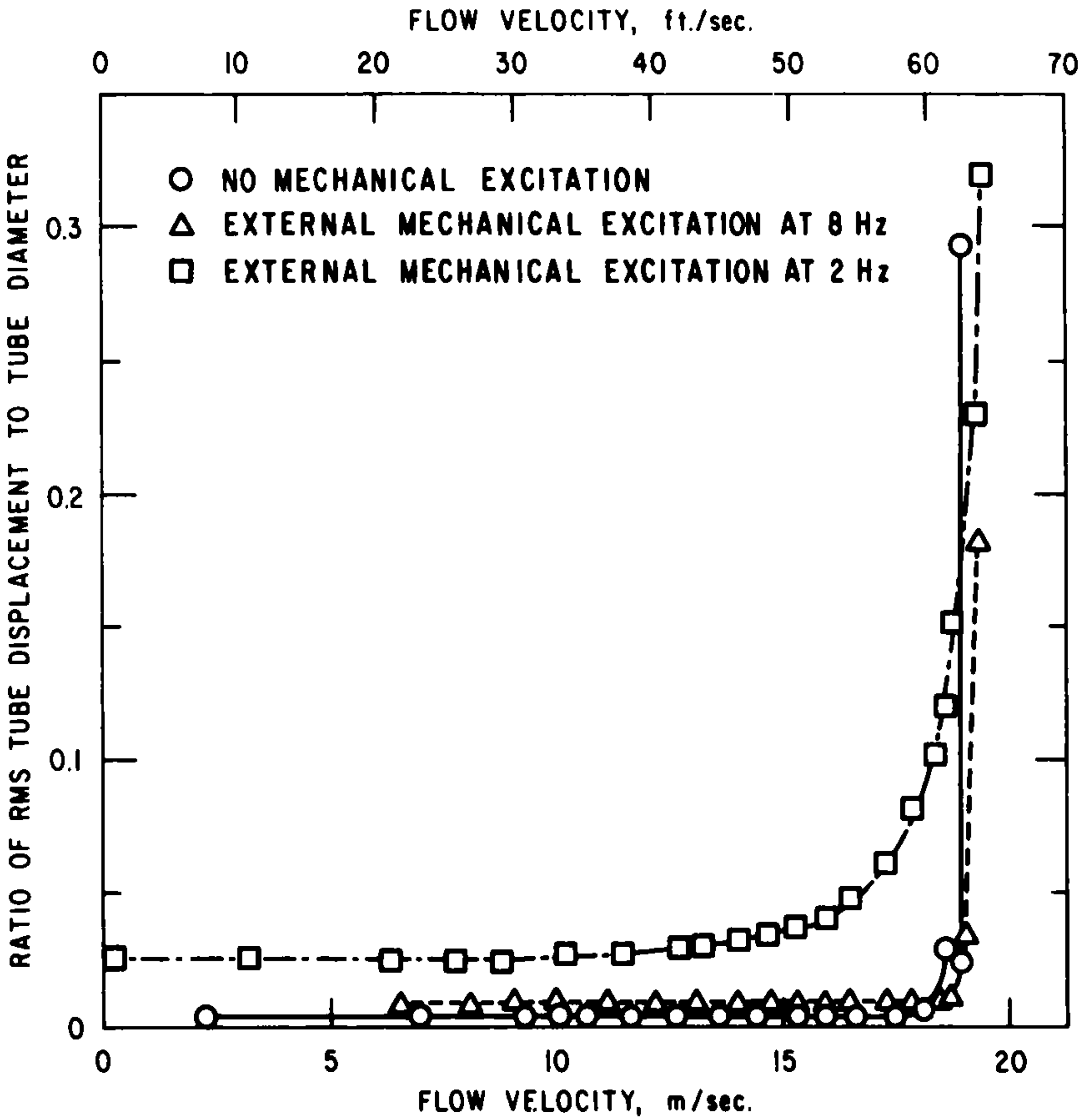

Fig. 28. RMS Tube Displacements with External Mechanical Excitations for Test 5.2

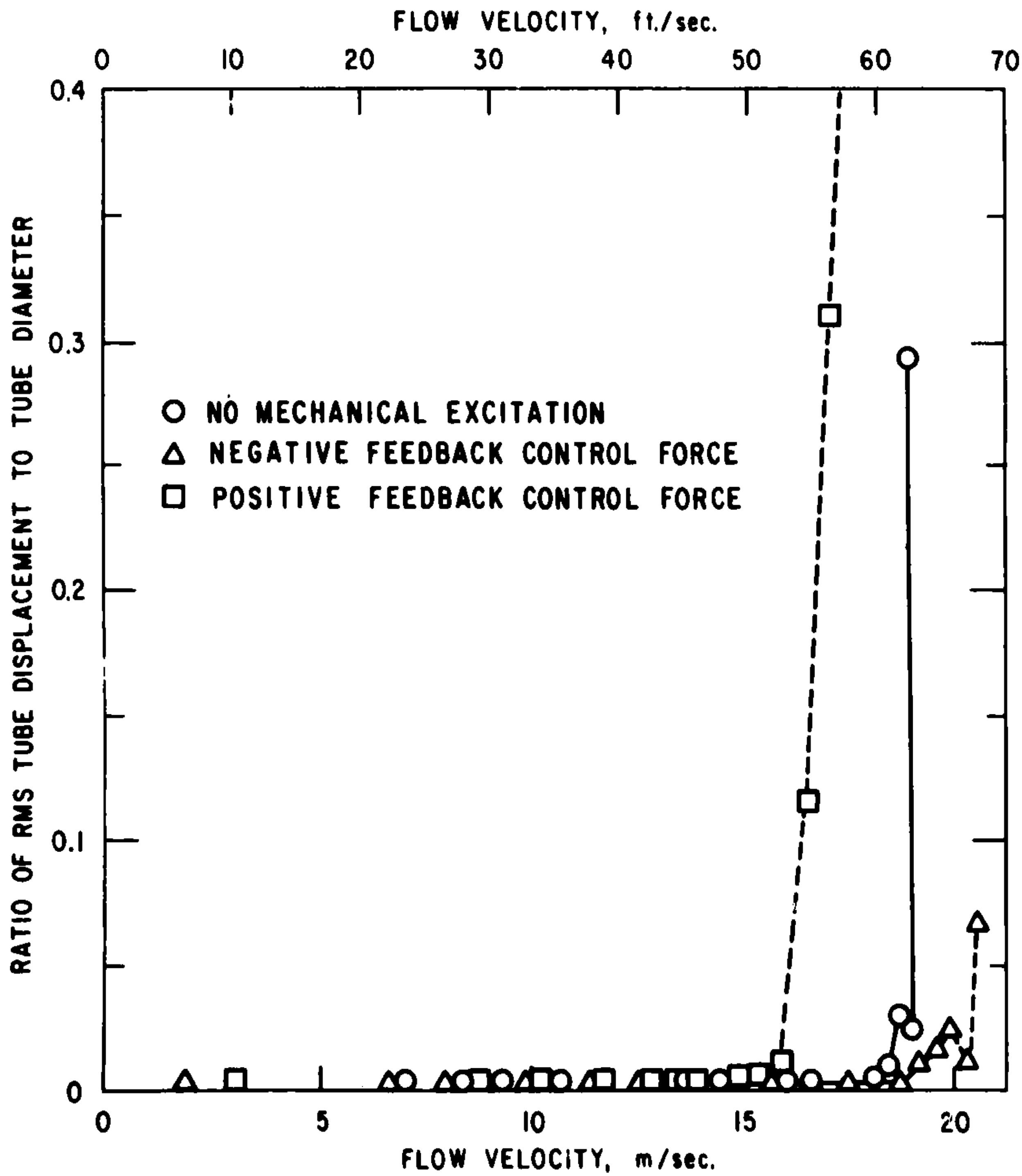

Fig. 29. RMS Tube Displacements with Feedback Control for Test 5.2

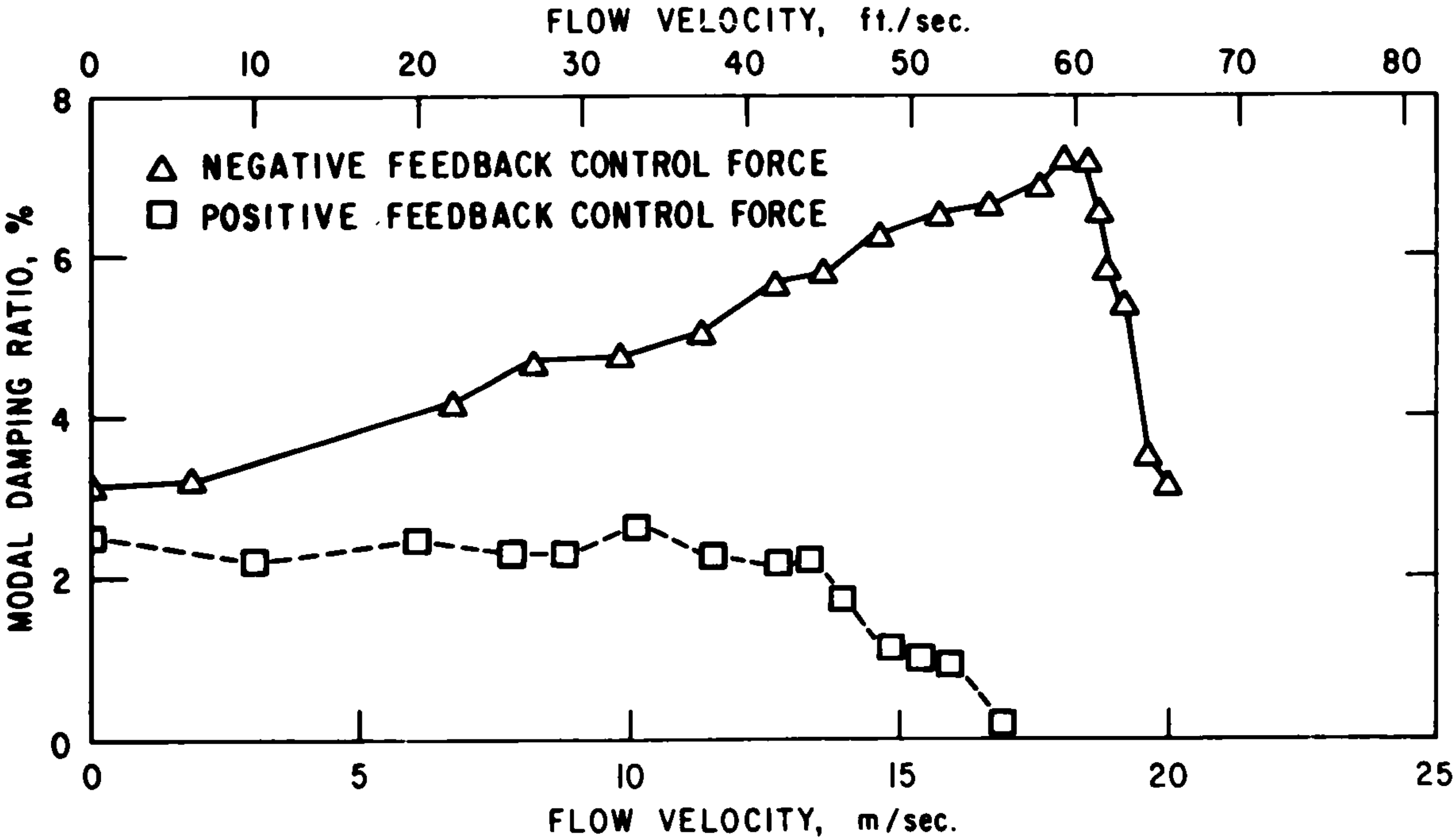

Fig. 30. Modal Damping Ratio of the Second Mode with Feedback Control for Test 5.2

The motion at the free end for Test 5.1 is relatively large. For control of stability, the control force is not very convenient to apply at the free end. This test illustrates the feasibility of feedback control.

F. Case 6: A Cantilevered Tube with a Concentrated Mass Attached at the Free End and a Concentrated Mass Movable along the Tube

The detailed characteristics of the tube response are not studied for this case. Figure 31 shows the critical flow velocity and the oscillation frequency at instability as a function of the location of the mass M_2. The lowest critical flow velocity occurs at ℓ/L equal to about 0.4.

The maximum flow velocity obtainable is about 27 m/s (88.6 ft/sec) for this tube. The lowest critical flow velocity is about 24.8 m/s (81.4 ft/sec) at ℓ/L equal to about 0.4. The available pump capacity is not large enough for a stability-control study. Therefore, no further study of this case is made.

IV. CONCLUSIONS AND DISCUSSIONS

This report presents the results of six cases for tubes conveying fluid. The data include the tube-response characteristics in the subcritical flow-velocity region, the critical flow velocity, and results from attempts to stabilize the tube by application of external and feedback control forces. The experimental data agree reasonably well with the published, linear, theoretical results and are consistent with other experimental observations.

Tube-response characteristics depend on the support conditions. The upstream end of the tube is fixed in all cases. The system may be classified into two groups according to the support at the downstream end:

1. Gyroscopic Conservative System: If the tube is not allowed to move at the downstream end, the tube cannot absorb fluid energy; for example, Case 3 is a gyroscopic conservative system.

2. Nonconservative System: If the downstream end is allowed to move, fluid energy can be absorbed by the tube; for example, Case 1 belongs to this type.

In the subcritical flow-velocity range, the tube responds differently for different types of boundary conditions. The two dominant fluid-force components are the fluid centrifugal force and the fluid Coriolis force. In a gyroscopic conservative system, the Coriolis force will produce a phase distortion for tube oscillations, so that there are no classical normal modes. The Coriolis force does not contribute to damping in this case. Therefore, the modal damping values do not increase because of the increase of flow velocity. In a nonconservative system, the Coriolis force will produce not only phase distortion, but also a dissipation mechanism for

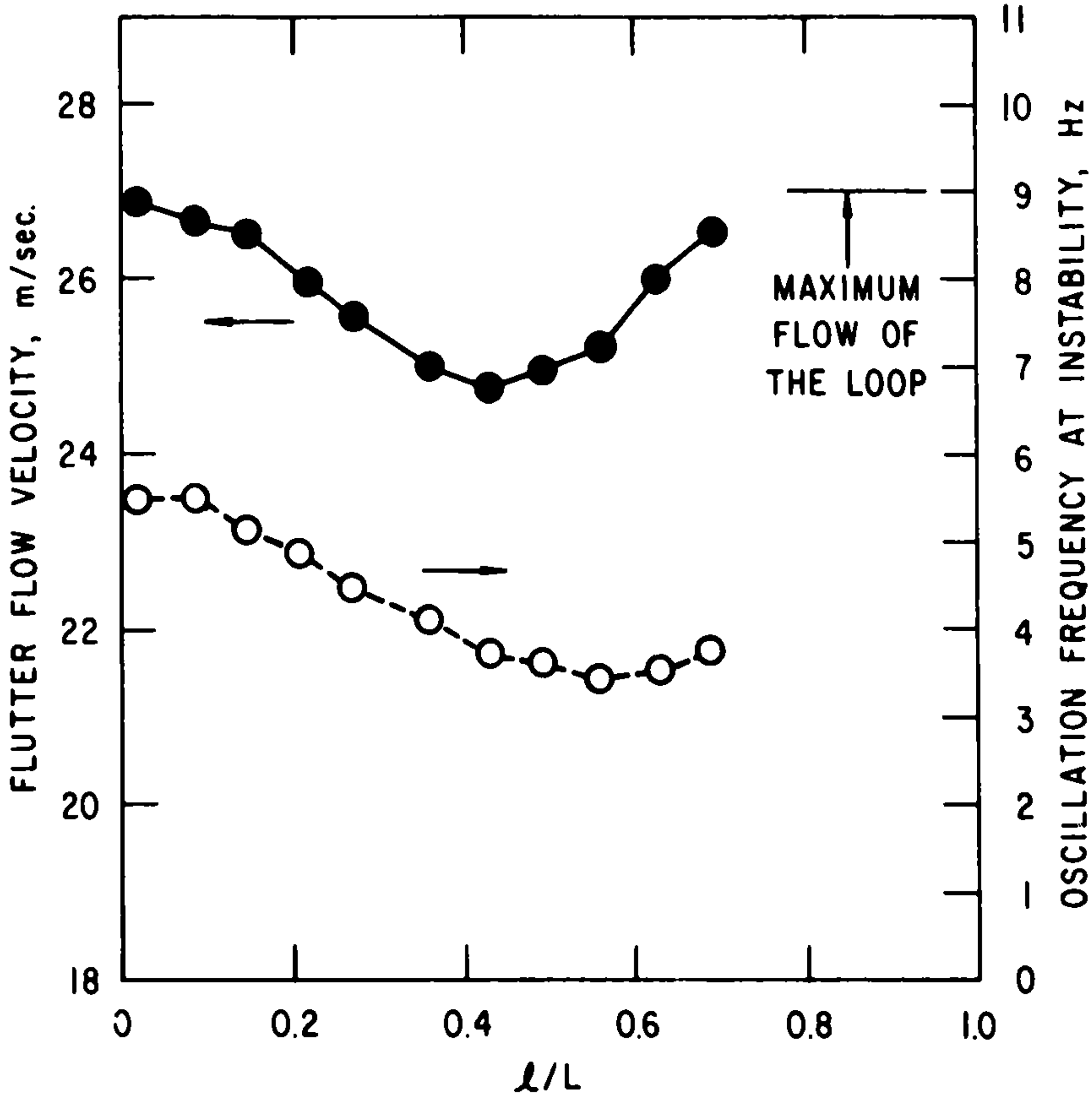

Fig. 31. The Critical Flow Velocity and Oscillation Frequency at Instability for Test 6

certain modes of tube oscillations. For example, in Case 1, the Coriolis force is a damping force for the first mode; the damping value of the first mode increases rapidly with the flow velocity. In fact, the tube is overly damped in the first mode, once the flow velocity reaches a certain value. Because of the Coriolis force, the system characteristics are very unpredictable; i.e., the tube responds contrary to what most other systems do. For example, adding an additional support normally will increase the rigidity of the system. However, providing an extra support to a cantilevered tube conveying fluid could reduce the "dynamic strength" of the tube.

In a gyroscopic system, the tube will lose stability by divergence. Once the tube becomes unstable by divergence, the nonlinear effects associated with relatively large tube displacement become important. The linear theory is not expected to be applicable beyond the critical flow velocity associated with divergence. Based on the nonlinear theory, it has been shown that a tube in a gyroscopic conservative configuration cannot flutter.[21] The experimental data obtained in this study, as well as published results,[5] are in agreement with these theoretical results. However, several investigators, based on the linear theory, have concluded that flutter is possible for a gyroscopic system.[22,23] Although flutter can occur in other structures, such as plates and shells submerged in flow, the gyroscopic conservative system consisting of a tube conveying fluid appears not to lose stability by flutter.

Except for Case 3, the other cases are examples of nonconservative systems. In contrast to a gyroscopic conservative system, a nonconservative system may be subjected to flutter and/or divergence types of instability. This study demonstrated that Cases 1, 5, and 6 lose stability by flutter. No divergence type of instability is observed. In Case 2, the instability will depend on the magnitude of the spring constant; because of the nonlinear behavior of the spring, the transition between the two different instability mechanisms cannot be demonstrated. In Case 4, the instability mechanisms depend on the location of the movable support. The transition from flutter for small ℓ/L to divergence for large ℓ/L is illustrated.

The critical flow velocity can be identified accurately for flutter using the tube displacement-flow velocity curve and/or frequency spectra of tube response. At instability, the tube displacement increases drastically with flow velocity and the tube responds at a single frequency. However, the critical flow velocity for divergence is much more difficult to define. This is attributed to the relatively large tube displacement caused by fluid centrifugal force in the subcritical flow-velocity range.

Case 5 is used to study the role of external and feedback control forces. Based on the experimental data, the external control force plays an insignificant role in controlling the tube stability. On the contrary, the feedback control force can stabilize or destabilize the tubes depending on the characteristics of the control force. This study has demonstrated the feasibility of controlling a nonconservative system. Since the nonconservative system under consideration possesses several dynamic characteristics that are intrinsic to some important engineering problems, such as the instability of laminar flow, the technique of stabilization might be useful for other applications.

ACKNOWLEDGMENTS

This work was performed under the sponsorship of the Office of Basic Energy Sciences, U.S. Department of Energy.

Acknowledgment is extended to G. S. Rosenberg and M. W. Wambsganss for thier support and encouragement, and E. L. Reiss of Northwestern University for his consultation.

REFERENCES

1. Chen, S. S., "Parallel-Flow-Induced Vibrations and Instability of Cylindrical Structures," Shock Vib. Dig. 6(10), 2-12 (1974).

2. Blevins, R. D., "Flow-Induced Vibration," Van Nostrand Reinhold Co., 1977.

3. Long. R. H., "Experimental and Theoretical Study of Transverse Vibration of a Tube Containing Flowing Fluid," Trans. ASME, J. Appl. Mech. 77, 65-68 (1955).

4. Gregory, R. W., and Paidoussis, M. P., "Unstable Oscillation of Tubular Cantilevers Containing Fluid, II - Experiments," Proc. Roy. Soc. A 293, 528-542 (1961).

5. Dodds, H. L., and Runyan, H. L., "Effect of High-Velocity Fluid Flow on the Bending Vibrations and Static Divergence of a Simply Supported Pipe," NASA-TN-D-2870, 1965.

6. Greenwald, A. S., and Dugundji, J., "Static and Dynamic Instabilities of a Propellant Line," MIT, AFOSR Scientific Report, AFOSR 67-1395, May 1967.

7. Naguleswaran, S., and Williams, C. J. H., "Lateral Vibration of a Pipe Conveying a Fluid," J. Mech. Eng. Sci. 10(3), 228-238 (1968).

8. Paidoussis, M. P., "Dynamics of Tubular Cantilevers Conveying Fluid," J. Mech. Eng. Sci. 12(2), 85-103 (1970).

9. Hill, J. L., and Swanson, C. P., "Effect of Lumped Masses on the Stability of Fluid Conveying Tubes," Trans. ASME, J. Appl. Mech. 92, 494-498 (1970).

10. Liu, H. S., and Mote, C. D., "Dynamic response of Pipes Transporting Fluids," Trans. ASME, J. Eng. Ind. 96, 591-596 (1974).

11. Paidoussis, M. P., and Issid, N. T., "Experiments on Parametric Resonance of Pipes Containing Flow," ASME J. Appl. Mech. 43, 198-202 (1976).

12. Becker, M., Hauger, W., and Winzen, W., "Exact Stability Analysis of Uniform Cantilevered Pipes Conveying Fluid or Gas," Arch. Mech. 30(6), 757-768 (1978).

13. Hannoyer, M. J., and Paidoussis, M. P., "Dynamics of Slender Tapered Beam with Internal or External Axial Flow; Part 2: Experiments," ASME J. Appl. Mech. 46, 52-57 (1979).

14. Shilling, R., and Lou, Y. K., "An Experimental Study on the Dynamic Response of a Vertical Cantilever Pipe Conveying Fluid," Trans. ASME, J. Energy Resources Technol. 102, 129-135 (1980).

15. Benjamin, T. B., "Dynamics of a System of Articulated Pipes Conveying Fluid: II. Experiments," Proc. Roy. Soc. A 261, 487-499 (1961).

16. Bohn, M. P., and Herrmann, G., "Instabilities of a Spatial System of Artic·'ated Pipes Conveying Fluids," ASME J. Fluids Eng. 86, 289-296 (1974).

17. Paidoussis, M. P., and Deksnis, E. B., "Articulated Models of Cantilevers Conveying Fluid: The Study of a Paradox," J. Mech. Eng. Sci. 12(4), 288-300 (1970).

18. Strumolo, G., and Reiss, E. L., "Poiseuille Channel Flow with Driven Walls," to appear J. Fluid Mechanics.

19. Gregory, R. W., and Paidoussis, M. P., "Unstable Oscillation of Tubular Cantilevers Conveying Fluid, I - Theory," Proc. Roy. Soc. A 293, 512-527 (1961).

20. Chen, S. S., "Flow-Induced Instability of an Elastic Tube," ASME Paper No. 71-Vibr-39 (1971).

21. Holmes, P. J., "Pipes Supported at Both ends Cannot Flutter," Trans. ASME, J. Appl. Mech. 45, 619-622 (1978).

22. Paidoussis, M. P., "Flutter of Conservative System of Pipes Conveying Incompressible Fluid," J. Mech. Eng. Sci. 17, 19-25 (1975).

23. Weaver, D. S., "On the Non-Conservative Nature of Gyroscopic Conservative Systems," J. Sound Vib. 36(3), 435-437 (1974).

Distribution for ANL-83-18

Internal:

E. S. Beckjord
C. E. Till
R. S. Zeno
P. R. Huebotter
G. S. Rosenberg
M. W. Wambsganss (20)
A. R. Brunsvold
B. L. Boers
S. S. Chen (15)
H. Halle
J. A. Jendrzejczyk (20)
T. M. Mulcahy
M. P. Agresta
M. Weber
R. A. Valentin
S. H. Fistedis
ANL Patent Dept.
ANL Contract File
ANL Libraries
TIS Files (6)

External:

DOE-TIC, for distribution per UC-34 (98)
Manager, Chicago Operations Office, DOE
Director, Technology Management Div., DOE-CH
E. Gallagher, DOE-CH
Components Technology Division Review Committee:
  A. A. Bishop, U. Pittsburgh
  F. W. Buckman, Consumers Power Co.
  R. Cohen, Purdue U.
  R. A. Greenkorn, Purdue U.
  W. J. Jacobi, Westinghouse Electric Corp., Pittsburgh
  E. E. Ungar, Bolt Beranek and Newman, Inc., Cambridge, Mass.
  J. Weisman, U. Cincinnati